Squeezed atomic states and projection noise in spectroscopy

D. J. Wineland, J. J. Bollinger, and W. M. Itano
Time and Frequency Division, National Institute of Standards and Technology, Boulder, Colorado 80303

D. J. Heinzen
Physics Department, University of Texas, Austin, Texas 78712
(Received 11 January 1994)

We investigate the properties of angular-momentum states which yield high sensitivity to rotation. We discuss the application of these "squeezed-spin" or correlated-particle states to spectroscopy. Transitions in an ensemble of N two-level (or, equivalently, spin-$\frac{1}{2}$) particles are assumed to be detected by observing changes in the state populations of the particles (population spectroscopy). When the particles' states are detected with 100% efficiency, the fundamental limiting noise is projection noise, the noise associated with the quantum fluctuations in the measured populations. If the particles are first prepared in particular quantum-mechanically correlated states, we find that the signal-to-noise ratio can be improved over the case of initially uncorrelated particles. We have investigated spectroscopy for a particular case of Ramsey's separated oscillatory method where the radiation pulse lengths are short compared to the time between pulses. We introduce a squeezing parameter ξ_R which is the ratio of the statistical uncertainty in the determination of the resonance frequency when using correlated states vs that when using uncorrelated states. More generally, this squeezing parameter quantifies the sensitivity of an angular-momentum state to rotation. Other squeezing parameters which are relevant for use in other contexts can be defined. We discuss certain states which exhibit squeezing parameters $\xi_R \simeq N^{-1/2}$. We investigate possible experimental schemes for generation of squeezed-spin states which might be applied to the spectroscopy of trapped atomic ions. We find that applying a Jaynes-Cummings–type coupling between the ensemble of two-level systems and a suitably prepared harmonic oscillator results in correlated states with $\xi_R < 1$.

PACS number(s): 03.65.Bz, 32.80.Pj, 06.30.Ft

I. INTRODUCTION

Intriguing features of quantum-mechanically correlated particles have become well known through the celebrated gedanken experiment of Einstein, Poldolsky, and Rosen (EPR) [1]. The most important of these have been demonstrated in "EPR-type" experiments which use correlated photons [2,3]. Optical fields have also provided the basis for numerous studies devoted to nonclassical harmonic-oscillator states such as squeezed states [4–7]. Demonstrated applications of squeezed optical states include the improvement of the signal-to-noise ratio in interferometers [8,9] and absorption spectroscopy [10]. By contrast, analogous studies of correlated or squeezed states of material particles are much less common, although they may lead to interesting new phenomena and applications.

First, it should be possible to generate squeezed states of harmonic oscillators which are not associated with the electromagnetic field. For example, as a result of the investigations devoted to the detection of gravitational waves with macroscopic antennas [11,12], it should be possible to generate squeezing in a material harmonic oscillator. In atomic physics, it has recently become possible to generate quantized states of motion for trapped atoms [13–16]. Therefore, it may also be possible to generate states of squeezed position or momentum for these atomic particles [15,17–21]. In addition, interesting studies have been devoted to the (phase) correlations between the different internal states within the same atomic particle (as opposed to correlations between different atomic particles). As a recent example, attention has been focused on atomic states which yield dispersion without absorption and "lasing without inversion" [22].

In this paper, we examine methods for the generation of quantum-mechanical correlations between the internal states of different atomic particles and investigate the use of these correlated atoms in spectroscopy. For example, consider atoms which have two internal levels with corresponding wave functions denoted $|1\rangle$ and $|2\rangle$. For the case of two such atoms, a and b, we will be interested in finding ways to generate correlated or "entangled" states of the form

$$\psi=[2\cosh(2\theta)]^{-1/2} \times(e^{-\theta}|2\rangle_a|2\rangle_b+e^{i\phi}e^{\theta}|1\rangle_a|1\rangle_b)\,, \tag{1}$$

where the subscripts refer to the atoms. (Here, the entanglement of the particle wave functions is evident because the total wave function cannot be written as the product of wave functions of the separate atoms). These states (for $\theta\rightarrow 0$, $\phi\rightarrow\pi$) are the correlated two-particle states discussed in Bohm's version of the Einstein, Podolsky, and Rosen experiment [23]. We will be interested in finding ways to generate these states and the analogous

correlated states for much larger numbers of particles.

If we make the connection between spin-$\frac{1}{2}$ particles and two-level systems [24], such states can also be called "squeezed-spin" states, where squeezing is defined in analogy to the squeezing for the electromagnetic field. Various aspects of spin squeezing have been considered previously [25–38]. For example, in the work of Ref. [26], the relationship between squeezing in a two-level system and squeezing of the radiation which is emitted by the two-level system is discussed. Reference [33] considers the generation of correlated or squeezed-spin states, in ensembles of two-level systems, by broadband squeezed vacuum radiation. The use of correlated states in interferometers has been discussed in Refs. [30] and [35]; these states correspond formally to the squeezing of angular-momentum operators.

We have found it useful to investigate spin squeezing in the context of spectroscopy. Part of the reason for this is that we were led to consider it as a natural outgrowth of our experiments on the spectroscopy of stored atomic ions [39,40]. Also, the squeezed-spin states that are useful in one physical context or application are not necessarily the ones of interest in another. For example, the form of spin squeezing discussed in Refs. [25–28,33] does not, as we describe below, appear to be relevant for the spectroscopy we describe here. However, the method of spectroscopy we assume is formally equivalent to the description of particle interferometry discussed earlier [30,35]. Therefore, the same form of squeezed states is of interest in both contexts even though the states describe quite different physical systems and will require different interactions to be produced. The states of interest in spectroscopy and interferometry can be put in a more general context. In any system which can be represented by a net angular momentum **J**, the states we are interested in are those which give the highest angular resolution of $\langle \mathbf{J} \rangle$ about a particular axis.

In our experiments on stored ions [39], we detect atomic transitions by observing changes in atomic state population. Typically, we first localize an ensemble of N identical atoms in a trap, where N remains fixed throughout the experiments. We initially prepare each of the atoms in the same internal eigenstate, which we take to be state $|1\rangle$. We then apply (classical) radiation, which we will call the clock radiation, to the atoms. The clock radiation has a frequency that drives the atoms from state $|1\rangle$ to another state, designated state $|2\rangle$. After application of this radiation, an atom is, in general, in a coherent superposition state $c_1|1\rangle+c_2|2\rangle$, where $|c_1|^2+|c_2|^2=1$. We assume that relaxation of states 1 and 2 is negligible; this is usually a good approximation for stored atomic ions. We then detect the number of atoms in state $|1\rangle$ (or $|2\rangle$). In the detection process, we will find the atom to be in either state 1 or state 2; that is, the measurement can be thought of as projecting the atom into one of these states [40]. If we perform this preparation, irradiation, and detection many times, on average, we will detect $N_1=|c_1|^2N$ atoms to be in state 1. However, unless $|c_1|=1$ or 0, the number of atoms found in state 1 will fluctuate from measurement to measurement. We call these fluctuations "projection noise" [40]. They are given by

$$\Delta N_1=[N|c_1|^2(1-|c_1|^2)]^{1/2} .$$

Recently, we have reduced all other sources of noise in the experiments so that the signal-to-noise ratio is limited by projection noise [40]. In those experiments, ΔN_1 was given by the expression above. The ability to see the projection noise clearly was enabled by detecting a fixed number of atomic ions with high efficiency.

Projection noise is the fundamental limiting noise in spectroscopic experiments which detect transitions by monitoring changes in population on a fixed number of particles. In Ref. [38], we have investigated, theoretically, ways to increase the signal-to-noise ratio over what has been observed in Ref. [40], that is, when all of the atoms are initially prepared in the same internal eigenstate. This can be accomplished if we can initially prepare the atoms in particular correlated states.

The generation and detection of correlated atomic particle states by the methods described below is interesting because it would allow the investigation of squeezed states outside the domain of the electromagnetic field. Also, the increase in signal-to-noise ratio possible in spectroscopy with correlated states may be of practical interest. A dramatic example is the following: In atomic clocks which use uncorrelated atoms and are limited by projection noise, the signal-to-noise ratio is equal to $K(N\tau)^{1/2}$, where N is the number of atoms, τ is the total measurement time, and K is a constant. However, if the atoms are initially prepared in particular correlated states, the signal-to-noise ratio would be equal to $KN\tau^{1/2}$. Therefore an atomic clock using 10^{10} correlated atoms would yield the same precision in 1 s as an atomic clock using 10^{10} uncorrelated atoms taking 300 years. On a less ambitious scale, the attainment of modest squeezing should also be of practical significance. This is particularly true in measurements on atomic clocks where precision measurements take many days, weeks, or even years of averaging time. Therefore, for example, even if a squeezing of only $\xi_R=\frac{1}{2}$ is obtained (ξ_R defined in Sec. V A), a four-day measurement of a certain precision is reduced to a one-day measurement.

The purpose of the present paper is to extend the discussion of Ref. [38]. As in that paper, we will be interested in two things: (1) identifying states which reduce projection noise in the context of spectroscopy, and (2) how these states might be generated in an experiment. We will concentrate on squeezing in systems of trapped atoms because it is relevant to our experimental work and might be where such effects will first be demonstrated. However, the results are quite general, and the increase in signal-to-noise ratio will, in principle, apply to spectroscopy on any ensemble of two-level systems.

In Sec. II, we discuss the signal-to-noise ratio, or transition-frequency measurement uncertainty, in spectroscopic experiments which detect transitions by observing changes in level populations. As is often done, we use the analogy between spectroscopy on two-level systems and spectroscopy on spin-$\frac{1}{2}$ systems. This analogy will lead to a useful pictorial representation of the noise and

will make obvious what is desired of the squeezed-spin states. In Sec. III, we apply this analysis to a special case of spectroscopy which uses Ramsey's method of separated oscillatory fields [41]. Here, we discuss the connection between Ramsey's method and interferometry. In Sec. IV, we examine the signal-to-noise ratio when the particles are initially prepared in particular uncorrelated pure states. This is essentially a summary of the results of Ref. [40]. In Sec. V, we show that some correlated particle states can be used in spectroscopy to increase the signal-to-noise ratio over that found in experiments which use uncorrelated particles. We define a squeezing parameter ξ_R which is relevant for these experiments and also show that ξ_R expresses the measurement sensitivity of an angular-momentum state to rotations. In Sec. VI, we discuss alternate definitions of spin squeezing. In Secs. VII and VIII, we investigate possible ways to generate the correlated states useful for spectroscopy. The difficulty will be in finding a practical scheme; we discuss some possibilities in Sec. VIII. Although the discussion will apply to an arbitrary number N of correlated particles, in many cases we will find it useful to illustrate various aspects of the squeezing for two particles.

II. POPULATION SPECTROSCOPY

We are interested in the spectroscopy of an ensemble of N identical two-level particles. We assume that transitions are detected by observing changes in the populations of the two levels after application of classical radiation. It will be convenient to use the fact that the dynamics of an individual two-level system interacting with radiation is the same as the dynamics of a spin-$\frac{1}{2}$ particle in a magnetic field [24]. This spin representation provides a simple pictorial way to follow the evolution of operators (or quantum states) under the influence of radiation. For an ensemble of particles, the spin representation also provides a simple way to visualize the noise in the measurement of populations, which will make obvious what is desired of the correlated states discussed in Sec. V.

Therefore, we begin by assuming that we have an ensemble of N identical particles, where N is fixed. Each particle has spin $\mathbf{S}$ where $S=\frac{1}{2}$. Associated with each spin is a magnetic moment $\boldsymbol{\mu}=\mu_0\mathbf{S}$. We assume that the particles are far enough apart that they do not overlap spatially, so that antisymmetrization (or symmetrization for integral-spin two-level particles) of the total wave function is unnecessary. We will also assume the particles are far enough apart that the direct dipole-dipole coupling or other direct interactions between particles can be neglected. Relaxation is assumed to be negligible. These are good approximations for many spectroscopic experiments on trapped atomic ions where the storage time is long, the background gas pressure is low, and the Coulomb repulsion between ions typically restricts particle separations to greater than 1 μm.

We apply a uniform external magnetic field $B_0\hat{\mathbf{z}}$ to the ensemble of spins, so the Hamiltonian for each particle is given by

$$H_0=-\boldsymbol{\mu}\cdot\mathbf{B}_0=\hbar\omega_0 S_z \ , \tag{2}$$

where $\omega_0\equiv-\mu_0 B_0/\hbar$. The eigenstates of this Hamiltonian are the $|m\rangle=|+\frac{1}{2}\rangle$ and $|-\frac{1}{2}\rangle$ states where $S_z|m\rangle=m|m\rangle$. The Heisenberg equation for $\mathbf{S}$ is

$$\partial\mathbf{S}/\partial t=\boldsymbol{\omega}_0\times\mathbf{S} \ , \tag{3}$$

where $\boldsymbol{\omega}_0\equiv\omega_0\hat{\mathbf{z}}$. If the particles are electrons, $\mu_0=g_J\mu_B$ where $g_J(\simeq-2)$ is the electron g factor and μ_B is the Bohr magneton. In this case, $\omega_0>0$ and $\mathbf{S}$ precesses in the $+\phi$ direction defined by Eq. (3). The upper and lower energy levels of this two-level system correspond to the $|+\frac{1}{2}\rangle$ and $|-\frac{1}{2}\rangle$ states, respectively.

In spectroscopy, we are interested in experimentally measuring ω_0. In our spin-$\frac{1}{2}$ model, the spectroscopy is essentially equivalent to NMR (nuclear magnetic resonance) on a spin-$\frac{1}{2}$ nucleus or ESR (electron spin resonance). In general, we might be interested in the case where the particles are first prepared in a mixed state. In this case, we would employ a density matrix treatment to describe the evolution of the system. However, since we will be concerned with maximizing the signal-to-noise ratio, we will assume that the particles are initially prepared in pure states with an average value of $\mathbf{S}$ which, for most of our discussion, we take to be aligned along the $\hat{\mathbf{z}}$ axis and denote $\langle S_z\rangle$. ($\langle A\rangle$ denotes the mean value of operator A.) We then apply (classical) radiation, which we call the spectroscopic or "clock" radiation, at a frequency ω (near ω_0), which changes $\langle S_z\rangle$. The measurement apparatus is configured to detect this change in $\langle S_z\rangle$. We assume the amplitude and duration of the radiation is adjusted so that $\langle S_z\rangle$ reverses sign when $\omega=\omega_0$.

An alternative method of performing spectroscopy is to observe the radiation transmitted through the sample of particles. If the intensity of the radiation is chosen appropriately, the maximum change in the transmitted intensity corresponds to the condition $\omega=\omega_0$. In some cases, for example, when N is large and the clock radiation weak, the fluctuations of the detected radiation (which limit the signal-to-noise ratio) are dominated by the fundamental quantum fluctuations of this radiation. In these experiments, the signal-to-noise ratio can be improved by using squeezed radiation [10,42–46]. Here, we have assumed that the radiation used for the spectroscopy is classical: that is, it is in a coherent state, and the number of photons in the radiation source is large enough that the quantum fluctuations in this radiation can be neglected. We assume all sources of technical noise (for example, fluctuations in the amplitude of the clock radiation caused by an unstable power supply) are also negligible. Since N is assumed constant, fluctuations in N, such as those which occur in an atomic-beam experiment, are absent.

In the measurement of S_z, we assume that each particle is projected into either the $|+\frac{1}{2}\rangle$ or $|-\frac{1}{2}\rangle$ eigenstate [40]. We will assume that we can detect which state the particle is measured to be in with 100% efficiency. With these assumptions, the noise in the measurements of S_z (for the same value of ω) from measurement to measurement is due to fluctuations in finding particles in either the $|+\frac{1}{2}\rangle$ or $|-\frac{1}{2}\rangle$ eigenstate.

It will be useful to use a formalism which treats the N particles as a combined quantum system. This has the advantage that, for one choice of basis states, it will provide a simple way to visualize the measurement noise when the particles are either uncorrelated or correlated. One possible choice of basis states is the set of direct-product states

$$|m_1,m_2,\ldots,m_N\rangle \equiv \prod_{i=1}^{N} |m_i\rangle \ , \tag{4}$$

where $|m_i\rangle$ is an eigenstate for the ith particle. However, we will use another common representation in which we define a collective angular-momentum operator

$$\mathbf{J}=\sum_{i=1}^{N} \mathbf{S}_i \ , \tag{5}$$

where $\mathbf{S}_i$ is the spin operator for the ith particle. The set of basis states we use are of the familiar form $|J,M\rangle$, which are linear combinations of the states in Eq. (4) [47,48]. For these states, $\mathbf{J}^2|J,M\rangle = J(J+1)|J,M\rangle$ and $J_z|J,M\rangle = M|J,M\rangle$.

Heisenberg picture

In the presence of the field $\mathbf{B}_0$, Eqs. (3) and (5) yield the Heisenberg equation for $\mathbf{J}$ (see Fig. 1):

$$\partial\mathbf{J}/\partial t = \boldsymbol{\omega}_0 \times \mathbf{J} \ . \tag{6}$$

The clock radiation is assumed to be a classical field, which rotates about the z axis, of the form

$$\mathbf{B}_1 = B_1 \left[\hat{\mathbf{x}} \cos(\omega t+\theta) + \frac{\omega_0}{|\omega_0|} \hat{\mathbf{y}} \sin(\omega t+\theta) \right] \ , \tag{7}$$

where $\omega \simeq \omega_0$ and the factor $\omega_0/|\omega_0|$ insures that $\mathbf{B}_1$ rotates in the same sense as $\boldsymbol{\omega}_0$. In general, B_1 is also a function of time. We assume that B_1 is switched rapidly between 0 and some constant value. In practice, the clock radiation may be an oscillating (magnetic) field which is perpendicular to $\mathbf{B}_0$. This oscillating magnetic field can be decomposed into two rotating fields: one which rotates at frequency ω [given by Eq. (7)], and the other rotating in the opposite sense. Usually the effects of the oppositely rotating field can be neglected [41] (rotating-wave approximation); we assume this to be the case here.

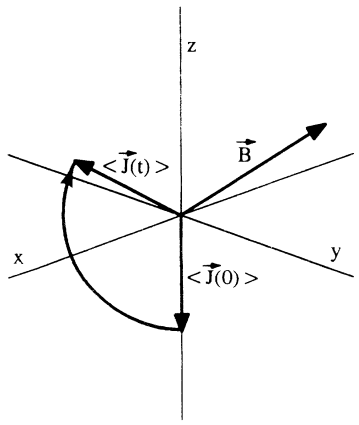

FIG. 1. Pictorial representation of the precession of the angular momentum $\mathbf{J}$ about an applied magnetic field $\mathbf{B}$. The angular momentum is assumed to have a net magnetic moment $\boldsymbol{\mu}=\mu_0\mathbf{J}$, where $\mu_0>0$ for the figure. The figure represents the motion of $\langle\mathbf{J}\rangle$ or the operator $\mathbf{J}$ in the Heisenberg representation [Eq. (6)].

To solve for the system evolution, it will be convenient to transform to a frame which rotates at frequency $\boldsymbol{\omega}$ [41,49]. In this frame of reference, the angular momentum $\mathbf{J}_r$ will interact with the effective field

$$\mathbf{B}=\hat{\mathbf{z}}B_r + B_1(\hat{\mathbf{x}}\cos\theta+\hat{\mathbf{y}}\sin\theta) \ ,$$

where

$$B_r \equiv B_0+\hbar\omega/\mu_0 = B_0(\omega_0-\omega)/\omega_0 \ .$$

Without loss of generality, we will assume $\theta=\pi/2$, in which case

$$\mathbf{B}=\hat{\mathbf{z}}B_r+\hat{\mathbf{y}}B_1 \ . \tag{8}$$

In this rotating frame, the Hamiltonian is given by

$$H_r = -\mu_0\mathbf{J}\cdot\mathbf{B} \equiv \hbar\boldsymbol{\omega}'\cdot\mathbf{J} \ , \tag{9}$$

where $\boldsymbol{\omega}' \equiv \omega_r\hat{\mathbf{z}}+\omega_1\hat{\mathbf{y}}$, $\omega_r \equiv -\mu_0 B_r/\hbar = \omega_0-\omega$, $\omega_1 \equiv -\mu_0 B_1/\hbar$, and $\mathbf{J}$ is now the angular momentum in the rotating frame. We have omitted an explicit subscript or superscript on $\mathbf{J}$ since only J_z will be measured and J_z is the same in both frames. The Heisenberg equation for $\mathbf{J}$ in the rotating frame is

$$\partial\mathbf{J}/\partial t = \boldsymbol{\omega}'\times\mathbf{J} \ . \tag{10}$$

In Fig. 1 we represent, pictorially, the time evolution of $\mathbf{J}$ (or $\langle\mathbf{J}\rangle$) when μ_0, $\omega_0-\omega>0$, $|\omega_0-\omega| \simeq |\omega_1|$, and $\langle\mathbf{J}(t=0)\rangle = -\hat{\mathbf{z}}|\langle J_z(0)\rangle|$.

As discussed by Ramsey [41], we could now transform to a second frame which rotates about $\mathbf{B}$ at a frequency $-\mu_0 B/\hbar$. In this frame, the effective magnetic field is 0 and therefore wave functions (in the Schrödinger picture) or operators (in the Heisenberg picture) remain constant. In this case, the system evolution is obtained by applying the appropriate rotation operators to the initial (laboratory) wave function or operators. In this paper, we will describe the system evolution in the first rotating frame corresponding to Eq. (10).

We will assume that, after application of the clock radiation, the detector measures the number of particles N_+ in the $|+\frac{1}{2}\rangle$ state. In the Heisenberg picture, this is given by the operator

$$N_+(t_f) = J_z(t_f) + JI \ , \tag{11}$$

where I is the identity operator and t_f is the "final" time corresponding to the time just after the clock radiation is applied. For a particular value of ω, we denote a single measurement of N_+ by $(N_+)_1$, and the average of M measurements of N_+ by $(N_+)_M$. By making measurements of $(N_+(t_f))_M$ for various values of ω, we obtain a resonance curve as a function of ω. To find ω_0, we could

fit this resonance curve to a particular function. The uncertainty in the determination of ω_0 would result from the noise in our measurements of $(N_+(t_f))_M$ at each value of ω.

In many cases of experimental interest, we can assume the resonance curve is symmetric about ω_0; this is true for the spin-$\frac{1}{2}$ example discussed here when $\langle \mathbf{J}(t=0)\rangle = -\hat{\mathbf{z}}|\langle J_z(0)\rangle|$. In this case, rather than fitting to the entire resonance curve, it will, in general, be advantageous to measure N_+ at particular values of ω which minimize the uncertainty in the apparent position (as a function of ω) of the curve. For a particular value of ω, the deviation of the apparent position of the curve from the true curve $\langle N_+ \rangle$ is given by

$$\delta\omega_M = [(N_+)_M - \langle N_+ \rangle]/(\partial\langle N_+ \rangle/\partial\omega) , \tag{12}$$

where the subscript M on $\delta\omega$ denotes the results for M measurements. The magnitude of the rms fluctuations of $\delta\omega$ for repeated measurements of $(N_+)_1$ at a particular value of ω is given by

$$\begin{aligned}|\Delta\omega| &= \Delta N_+(t_f)/|\partial\langle N_+ \rangle/\partial\omega| \\ &= \Delta J_z(t_f)/|\partial\langle J_z(t_f)\rangle/\partial\omega| ,\end{aligned} \tag{13}$$

where, as usual, for operator A, ΔA is the square root of the variance, $(\Delta A)^2 \equiv \langle A^2\rangle - \langle A\rangle^2$. If we make M measurements at a particular value of ω, the uncertainty in the value of ω_0 is reduced to $|\Delta\omega|_M = |\Delta\omega|(M)^{-1/2}$. Given N and t_f, our task in spectroscopy is to minimize $|\Delta\omega|$. Equivalently, since the signal-to-noise ratio can be defined as being proportional to $|\Delta\omega|^{-1}$, we therefore want to maximize signal-to-noise ratio.

If the exact form of the resonance curve were known, it would be necessary to measure the curve at only one frequency to determine the best value of ω_0. This is impractical since, for example, the height of the resonance curve ($\propto |\langle J_z(0)\rangle|$) depends on the exact value of B_1 and this may not be precisely determined. However, when the resonance curve is symmetric about ω_0, this difficulty is overcome, experimentally, by measuring two points on the resonance curve, at frequencies $\omega_A > \omega_0$ and $\omega_B < \omega_0$ where $\omega_A - \omega_0 \simeq \omega_0 - \omega_B$. If $\langle N_+(\omega=\omega_A)\rangle = \langle N_+(\omega=\omega_B)\rangle$, then $(\omega_A+\omega_B)/2 = \omega_0$. In practice, we approximate this condition with a servo mechanism [50].

III. POPULATION SPECTROSCOPY USING THE RAMSEY METHOD

In order to illustrate the basic ideas behind the improvement in signal-to-noise ratio using correlated states, we will examine $|\Delta\omega|$ for a special case of the resonance method due to Ramsey [41]. This is an important case to analyze because, experimentally, for a given time t_f in which to apply the clock radiation, the narrowest linewidths are obtained with this method. The Ramsey method [41] breaks the resonance period ($t=0\rightarrow t_f$) into three parts. In the special case discussed here, during the first part of the resonance period, B_1 is nonzero and constant with value B_{10} from time $t=0$ to $t=t_{\pi/2}$ such that $\Omega_R t_{\pi/2} = \pi/2$ and $\Omega_R \gg |\omega-\omega_0|$, where $\Omega_R \equiv \mu_0 B_{10}/\hbar$ is usually called the Rabi frequency. At time $t_{\pi/2}$, B_1 is reduced to zero. After an additional time T, B_1 is again made equal to B_{10} for a time $t_{\pi/2}$ and then reduced to zero. We will assume that B_1 is switched between zero and B_{10} in a time much less than $t_{\pi/2}$ in which case $t_f = 2t_{\pi/2} + T$. We make the further assumption that $T \gg t_{\pi/2}$.

With these assumptions, and assuming $\langle \mathbf{J}(0)\rangle = -\hat{\mathbf{z}}|\langle J_z(0)\rangle|$, during the first part of the Ramsey period, that is, during the first "Ramsey pulse," $\mathbf{B} = B_r\hat{\mathbf{z}} + B_{10}\hat{\mathbf{y}} \simeq B_{10}\hat{\mathbf{y}}$. In the rotating frame, from Eq. (10), $\mathbf{J}$ (or $\langle \mathbf{J}\rangle$) precesses around the $\hat{\mathbf{y}}$ axis until it lies along the $\hat{\mathbf{x}}$ axis at which point B_1 is reduced to 0 [Fig. 2(a)]. From time $t=t_{\pi/2}$ to $t_{\pi/2}+T$, $\mathbf{J}$ precesses around $\mathbf{B} = B_r\hat{\mathbf{z}}$ so that $\mathbf{J}(t_{\pi/2}+T)$ lies at an angle $(\omega_0-\omega)T$ with respect to $\hat{\mathbf{x}}$ but still in the x-y plane [Fig. 2(b)]. In the third part of the Ramsey period, from time $t_{\pi/2}+T$ to $2t_{\pi/2}+T=t_f$, $\mathbf{J}$ again precesses around $B_{10}\hat{\mathbf{y}}$ so that at time t_f it lies in the y-z plane [Fig. 2(c)]. At this point, N_+ or, equivalently, J_z is measured [Eq. (11)]. We have

$$\langle N_+(t_f)\rangle = J - \langle J_z(0)\rangle\cos(\omega_0-\omega)T , \tag{14}$$

which is the Ramsey resonance curve for $T \gg t_{\pi/2}$ [51]. In general, we can choose $B_{10} = \pm(n+\frac{1}{2})\pi\hbar/(\mu_0 t_{\pi/2})$ ($n=0,1,2,3,\ldots$) with the same result [52]. Other choices of B_{10} will result in smaller values of $|\partial\langle J_z(t_f)\rangle/\partial\omega|$. For brevity we will assume $n=0$.

Application of the Ramsey fields corresponds, in the Heisenberg picture in the rotating frame, to the transformations

$$J_x(t_f) = -J_x(0) , \tag{15}$$

$$J_y(t_f) = J_z(0)\sin\omega_r T + J_y(0)\cos\omega_r T , \tag{16}$$

and

$$J_z(t_f) = -J_z(0)\cos\omega_r T + J_y(0)\sin\omega_r T , \tag{17}$$

where $\omega_r \equiv \omega_0 - \omega$. Therefore, in general, from Eqs. (11) and (15)–(17),

$$\begin{aligned}\langle N_+(t_f)\rangle &= J - \langle J_z(0)\rangle\cos\omega_r T + \langle J_y(0)\rangle\sin\omega_r T \\ &= J - [\langle J_z(0)\rangle^2 + \langle J_y(0)\rangle^2]^{1/2} \\ &\quad \times \cos\{\omega_r T + \tan^{-1}[\langle J_y(0)\rangle/\langle J_z(0)\rangle]\}\end{aligned} \tag{18}$$

and

$$\begin{aligned}|\Delta\omega|^2 = \{&\Delta J_z(0)^2\cos^2\omega_r T + \Delta J_y(0)^2\sin^2\omega_r T \\ &+ [\langle J_y(0)\rangle\langle J_z(0)\rangle - \tfrac{1}{2}\langle J_z(0)J_y(0) + J_y(0)J_z(0)\rangle]\sin 2\omega_r T\}[T(\langle J_z(0)\rangle\sin\omega_r T + \langle J_y(0)\rangle\cos\omega_r T)]^{-2} .\end{aligned} \tag{19}$$

We see from Eq. (18) that the resonance curve is not symmetric about ω_0 unless $\langle J_y(0)\rangle=0$. Even when $\langle J_y(0)\rangle=0$, for initial states where

$$\langle J_z(0)J_y(0)+J_y(0)J_z(0)\rangle\neq 0 ,$$

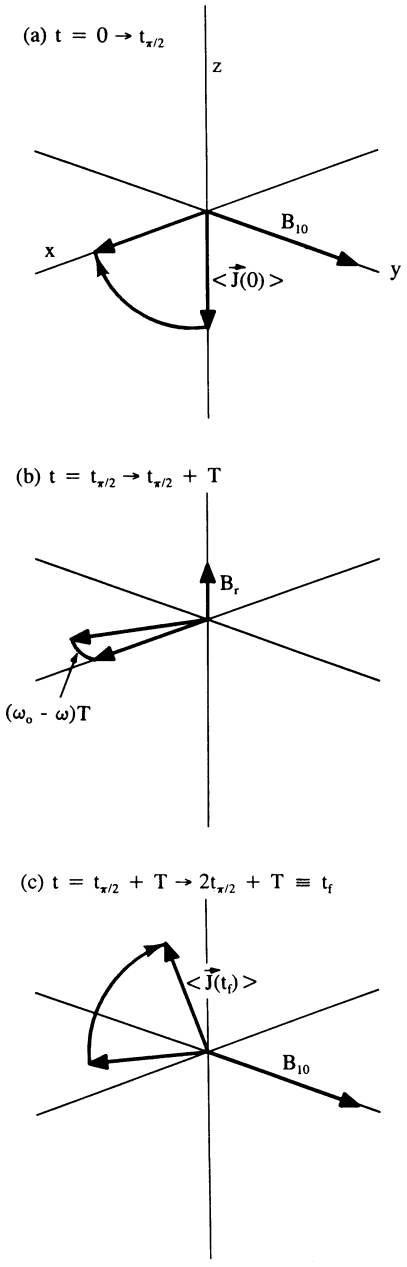

FIG. 2. Pictorial representation of the three parts of the Ramsey separated-field method. The figures apply to a frame which rotates with the applied time-varying field given by Eq. (7) of the text. Part (a) shows the precession of **J** during the first "$\pi/2$ pulse." In (b), **J** precesses about the residual field $\mathbf{B}_r$. In (c), **J** rotates into the y-z plane under the application of the second $\pi/2$ pulse. We assume $|\mathbf{B}_r|\ll|\mathbf{B}_1|$ and $t_{\pi/2}\ll T$, so the total "interrogation time" $t_f=t_{\pi/2}+T+t_{\pi/2}\simeq T$. After the second $\pi/2$ pulse, $J_z(t_f)$ is measured; this yields the signal used in spectroscopy [Eqs. (11) and (14)].

the quantum noise on the Ramsey curve $\Delta N_+(t_f)$ $[=\Delta J_z(t_f)]$ is not symmetric about ω_0. This is not necessarily a problem for finding the best value of ω_0 since the contribution to the noise in a measurement of $N_+(\omega_A)-N_+(\omega_B)$ from this term drops out. If we assume

$$\langle J_z(0)J_y(0)+J_y(0)J_z(0)\rangle=\langle J_y(0)\rangle=0 ,$$

then

$$|\Delta\omega|^2=\frac{\Delta J_z(0)^2\cos^2\omega_r T+\Delta J_y(0)^2\sin^2\omega_r T}{T^2\langle J_z(0)\rangle^2\sin^2\omega_r T} . \tag{20}$$

In practice, some additional noise will be present in the measurement of N_+. Assuming that this noise is uncorrelated with the projection noise and with ω, the noise $\Delta N_+(t_f)$ in the measurement of N_+ must be replaced by $[\Delta N_+(t_f)^2+\Delta N_{\rm add}^2]^{1/2}$, where $\Delta N_{\rm add}$ is the rms value of the added noise. From Eq. (13), Eq. (20) becomes

$$|\Delta\omega|^2=\frac{\Delta J_z(0)^2\cos^2\omega_r T+\Delta J_y(0)^2\sin^2\omega_r T+\Delta N_{\rm add}^2}{T^2\langle J_z(0)\rangle^2\sin^2\omega_r T} . \tag{21}$$

Equation (21) shows that with $\Delta J_z(0)\neq 0$ and/or $\Delta N_{\rm add}\neq 0$, $|\Delta\omega|$ is minimized for the choices $\omega_0-\omega=\pm(n+\frac{1}{2})\pi/T$ $(n=0,1,2,3,\ldots)$ [53].

Independent of the values of $\Delta J_z(0)$ and $\Delta N_{\rm add}$, $|\Delta\omega|$ is minimized for $n=0$ or equivalently for $\omega_0-\omega=\pm\pi/(2T)$. These values of $\omega_0-\omega$ will be assumed throughout the remainder of the paper except where noted. In other words, we will measure the resonance curve at frequencies $\omega_A=\omega+\pi/(2T)$ and $\omega_B=\omega-\pi/(2T)$ where $|\omega-\omega_0|$ is assumed to be much less than $\pi/(2T)$. In terms of Eq. (14), this means that we measure N_+ at two frequencies corresponding to the half-intensity points on the central lobe of the Ramsey resonance curve. With this assumption on ω_A and ω_B, $|\Delta\omega|$ is independent of $\langle J_z(0)J_y(0)+J_y(0)J_z(0)\rangle$ and $\langle J_y(0)\rangle$.

In the remainder, we will assume $\Delta N_{\rm add}\ll\Delta J_y(0)$, in which case we end up with a simple expression for $|\Delta\omega|$ [38]:

$$|\Delta\omega|=\Delta J_y(0)/[T|\langle J_z(0)\rangle|] . \tag{22}$$

We can represent $\Delta N_+(t_f)$ $[=\Delta J_z(t_f)]$ pictorially. More generally, we can represent ΔJ_x, ΔJ_y, and ΔJ_z by an "error spheroid" (or error ellipsoid) [28] which lies at the end of the vector **J** and whose dimensions are given by ΔJ_x, ΔJ_y, and ΔJ_z. This is shown schematically in Fig. 3 for the case $\langle\mathbf{J}\rangle=-|\langle\mathbf{J}\rangle|\hat{\mathbf{z}}$. (In Refs. [29], [36], [38], and [40], ΔJ_x and ΔJ_y are represented as semimajor axes of an ellipse placed at the end of, and perpendicular to, $\langle\mathbf{J}\rangle$.) The pictorial representation shown in Fig. 3 will be useful for the method of spectroscopy described above, but is somewhat limited. For example, certain states with $\langle\mathbf{J}\rangle=-|\langle\mathbf{J}\rangle|\hat{\mathbf{z}}$ and $\langle J_zJ_y+J_yJ_z\rangle\neq 0$ might have, in a (primed) coordinate system rotated with respect to the spheroid shown in Fig. 3, a value of $\Delta J_z'<\Delta J_x,\Delta J_y,\Delta J_z$. This state might be more appropriately represented with an error spheroid which is tilted

with respect to the one shown in Fig. 3. Also, when $\langle \mathbf{J} \rangle = -|\langle \mathbf{J} \rangle|\hat{\mathbf{z}}$, and $|\langle \mathbf{J} \rangle| \neq J$, the distribution of measured values of J_z is not symmetric about $\langle J_z(0) \rangle$. Therefore the error spheroid should be distorted along z. A more accurate representation is given by plotting the probability distributions for $N_+(t_f)$ which are, in general, asymmetric about $\langle N_+(t_f) \rangle$ (see, for example, Fig. 3 of Ref. [40]). Other pictorial methods can be used to describe the probability distribution for measurements of N_+ or $\mathbf{J}$. For example, Ref. [37] provides a way of visualizing correlated or squeezed-spin states through the use of Wigner functions for angular momentum.

Since we have chosen $\omega_0 - \omega = \pm\pi/(2T)$, the evolution of the error spheroid at various times during the Ramsey period has a simple representation, as shown in Fig. 4. Since the three parts of the Ramsey period correspond to $\pi/2$ rotations about $B_{10}\hat{\mathbf{y}}$, $B_r\hat{\mathbf{z}}$, and $B_{10}\hat{\mathbf{y}}$, respectively, the evolution of the variances is particularly easy to follow. In Fig. 4(d), we plot $\langle N_+(t_f) \rangle$ as a function of ω

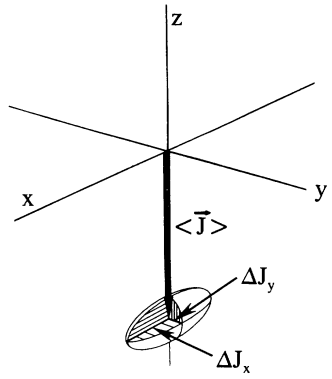

FIG. 3. Pictorial representation of the fluctuations in the measured values of J_x, J_y, and J_z. In this figure $\langle \mathbf{J} \rangle$ is taken to point along the negative z axis. The dimensions of the axes of the spheroid are ΔJ_x, ΔJ_y, and ΔJ_z where $\Delta J_i^2 \equiv \langle J_i^2 \rangle - \langle J_i \rangle^2$ and $i = x,y,z$.

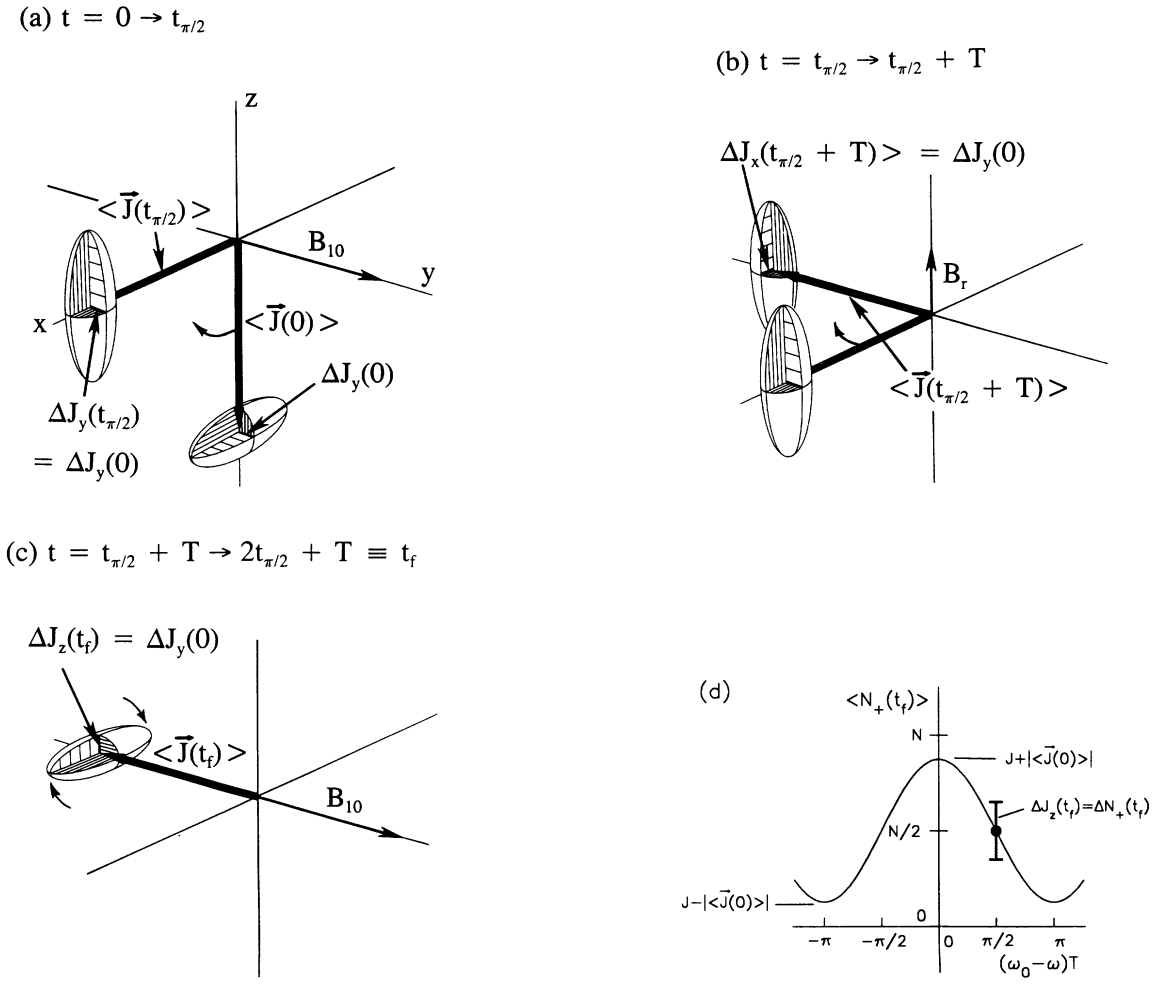

FIG. 4. Pictorial representation of the evolution of $\langle \mathbf{J} \rangle$ and the fluctuations at various parts of the Ramsey method for the condition $\omega_0 - \omega = \pi/2T$. From these figures we see that the fluctuations in $N_+(t_f)$ are given by $\Delta J_z(t_f)$ or $\Delta J_y(0)$. In part (d) of the figure, we show the point on the Ramsey curve corresponding to $\omega_0 - \omega = \pi/2T$. ΔN_+ represents the rms fluctuations for repeated measurements of N_+ for $\omega_0 - \omega = \pi/2T$. For part (d), we have assumed that the initial state is such that $\langle \mathbf{J} \rangle$ is aligned with the negative z axis but $|\langle \mathbf{J} \rangle| < J$.

[Eq. (14)], the particular point on the resonance curve corresponding to $\omega_0-\omega=\pi/(2T)$, and the corresponding value of the uncertainty in the measurement $\Delta N_+(t_f)=\Delta J_z(t_f)=\Delta J_y(0)$.

A. Schrödinger picture

In some cases, it will be useful to represent the system dynamics in the Schrödinger picture. As before, we assume we are in the rotating frame in which $\mathbf{B}_1$ is stationary [Eq. (8)]. In this frame, operators will now be assumed to be time independent, and the wave function evolves according to

$$\Psi(t)=U(t,0)\Psi(0) , \tag{23}$$

where the evolution operator U is the solution to the equation $i\hbar\, dU/dt=H_r U$ [54].

In the case of two particles ($J=1$), for example, following the application of the Ramsey fields, we have

$$U(t_f,0)=\frac{1}{2}\begin{bmatrix} (\cos\omega_r T-1) & -i\sqrt{2}\sin\omega_r T & (\cos\omega_r T+1) \\ i\sqrt{2}\sin\omega_r T & -2\cos\omega_r T & i\sqrt{2}\sin\omega_r T \\ (\cos\omega_r T+1) & -i\sqrt{2}\sin\omega_r T & (\cos\omega_r T-1) \end{bmatrix} , \tag{24}$$

where we use the notation

$$\psi=a|1,1\rangle+b|1,0\rangle+c|1,-1\rangle\equiv\begin{bmatrix} a \\ b \\ c \end{bmatrix} . \tag{25}$$

B. Comparison of Ramsey spectroscopy to interferometry

Yurke and co-workers [29–31] and others [55] have discussed the connection between a linear lossless passive device with two input and output ports and the SU(2) symmetry group. They construct abstract operators [56] $J_x=(a_1^\dagger a_2+a_2^\dagger a_1)/2$, $J_y=-i(a_1^\dagger a_2-a_2^\dagger a_1)/2$, $J_z=\frac{1}{2}(a_1^\dagger a_1-a_2^\dagger a_2)$, and $N=(a_1^\dagger a_1-a_2^\dagger a_2)$, where $a_i^\dagger$ and a_i ($i=1,2$) are the creation and annihilation operators for particles (bosons or fermions) entering ports 1 or 2 of the device. For example, the system might be photons injected into a Mach-Zehnder interferometer. These abstract operators J_i ($i=x,y,z$) have the same mathematical properties as the angular-momentum operators and therefore the interferometer can be described in terms of this abstract spin space. N corresponds to the total number of particles entering both ports of the interferometer. Beam splitters and differential phase shifters between the two arms of the interferometer behave like rotations of the net spin operator. If we compare our case to this formalism for interferometers, the Ramsey spectroscopy we discuss is formally equivalent to a Mach-Zehnder interferometer where the two $\pi/2$ Ramsey pulses are identified with 50-50 beam splitters in the interferometer, and the phase shift incurred between the spin precession and the applied field in Ramsey spectroscopy corresponds to the differential phase shift between the interferometer arms. If we define the phase sensitivity in Ramsey spectroscopy as $\Delta\phi_R\equiv\Delta\omega T$, then the sensitivity of the Ramsey method is equivalent to the phase sensitivity of a Mach-Zehnder interferometer [see Eq. (13) of this paper and Eq. (3.16) of Ref. [29]]. Because of this connection, we wish to create the same form of correlated input states as desired for interferometers.

IV. SPECTROSCOPY OF UNCORRELATED PARTICLES

In this section, we consider the particles to be initially uncorrelated and independent. This case is treated in detail in Ref. [40]. Because the particles are assumed to be uncorrelated, the initial wave function can be written as a direct product

$$\psi(0)=\prod_{i=1}^{N}\psi_i(0) , \tag{26}$$

where $\psi_i(0)$ is the initial wave function for particle i.

By optical pumping techniques we can prepare atoms in energy eigenstates. Therefore, in our spin-$\frac{1}{2}$ model, we will be particularly interested in the case where all of the particles are initially prepared in, for example, the $\psi_i(0)=|-\frac{1}{2}\rangle$ state. In this case, the initial state is represented by the wave function

$$\psi(0)=|J=N/2,M=-N/2\rangle=\prod_{i=1}^{N}|-\tfrac{1}{2}\rangle_i , \tag{27}$$

which is a particular Dicke state [47]. For this state, $\langle J_z(0)\rangle=-J$, $\Delta J_z(0)=0$, $\Delta J_x(0)=\Delta J_y(0)=(J/2)^{1/2}$, and

$$\langle N_+(t_f)\rangle=\tfrac{1}{2}N[1+\cos(\omega-\omega_0)T] .$$

Equation (20) is identical to Eq. (22) for all values of ω_r since $\Delta J_z(0)=0$. In this case, the best value of ω_0 can be determined independent of where we measure on the resonance curve. This somewhat surprising result occurs because the quantum noise $\Delta N_+(t_f)$ is proportional to the signal slope $\partial\langle N_+\rangle/\partial\omega$ for all values of ω. Therefore, from Eq. (13), $|\Delta\omega|$ is independent of our choice of ω. The noise is equal to zero on the peaks and valleys of the Ramsey resonance curve because, there, we detect eigenstates of J_z [Fig. 5(a)]. Unfortunately, the sensitivity to frequency shifts is also equal to 0 on the peaks and valleys since the slope of the Ramsey curve is equal to 0. As discussed in the last section, if ΔN_{add} is not negligible, we

minimize $|\Delta\omega|$ if we operate at frequencies $\omega_0-\omega=\pm(n+\frac{1}{2})\pi/T$ ($n=0,1,2,3,\ldots$), and, for simplicity, we have restricted ourselves to $\omega_0-\omega=\pm\frac{1}{2}\pi/T$.

It is instructive to consider the evolution of the wave function in the Schrödinger picture. For example, for $J=1$, our initial wave function is $|1,-1\rangle$ [$a=b=0$, $c=1$ in Eq. (25)]. After application of the Ramsey fields we have from Eq. (24)

$$\begin{aligned}\psi(t_f)&=\tfrac{1}{2}(\cos\omega_r T+1)|1,1\rangle+\frac{i}{\sqrt{2}}\sin\omega_r T|1,0\rangle+\tfrac{1}{2}(\cos\omega_r T-1)|1,-1\rangle\\&=(\cos\omega_r T/2|+\rangle_1+i\sin\omega_r T/2|-\rangle_1)(\cos\omega_r T/2|+\rangle_2+i\sin\omega_r T/2|-\rangle_2)\\&=[U_1(t_f,0)|-\rangle_1][U_2(t_f,0)|-\rangle_2]=\psi_1(t_f)\psi_2(t_f)\ ,\end{aligned}\tag{28}$$

where, for simplicity, we write $|+\frac{1}{2}\rangle=|+\rangle$ and $|-\frac{1}{2}\rangle=|-\rangle$. The evolution operator for particle j satisfies $i\hbar dU_j/dt=H_rU_j$ and $\psi_j(t_f)$ is the wave function of particle j after being acted upon by the Ramsey fields. Therefore, the final wave function is the product of the final wave functions of the individual particles. The particles remain uncorrelated (or unentangled) after application of the Ramsey fields. This is true for the application of any form of the (classical) clock radiation and for any number of particles since the initial wave function is given by Eq. (26) and $U(t_f)=\prod U_j(t_f)$.

This case (when all particles are initially prepared in eigenstates) serves as a benchmark and has been realized experimentally. In Ref. [40], we reported spectroscopic experiments on $^9Be^+$ and $^{199}Hg^+$ ions where the signal-to-noise ratio was limited by the projection noise ΔN_+ in the measurements. In these experiments, the ions were prepared in eigenstates corresponding to the initial Dicke state given by Eq. (27) in our spin-$\frac{1}{2}$ model. For this case $|\Delta\omega|$ is given by Eq. (22), which we denote

$$|\Delta\omega|_{\rm DS}\equiv\frac{1}{T(2J)^{1/2}}=\frac{1}{TN^{1/2}}\ .\tag{29}$$

This value of $|\Delta\omega|$ is the minimum that can be obtained using uncorrelated states in the Ramsey spectroscopy described above. It is limited by the fundamental quantum fluctuations in the measurement. This limitation on $|\Delta\omega|$ observed in the experiments led us to consider the possibility of using correlated states for spectroscopy where even smaller values of $|\Delta\omega|$ might be obtained.

V. SPECTROSCOPY OF CORRELATED PARTICLES

A. Squeezing parameter for spectroscopy

Before we examine specific states which can reduce $|\Delta\omega|$ below $|\Delta\omega|_{\rm DS}$, we introduce a parameter which indicates the level of improvement. As described in the last section, $|\Delta\omega|_{\rm DS}$ provides a useful benchmark. Therefore we will define a "squeezing" parameter

$$\begin{aligned}\xi_R\equiv|\Delta\omega|/|\Delta\omega|_{\rm DS}&=(2J)^{1/2}\Delta J_z(t_f)/|\langle J_y(t_f)\rangle|\\&=(2J)^{1/2}\Delta J_y(0)/|\langle J_z(0)\rangle|\ ,\end{aligned}\tag{30}$$

where $|\Delta\omega|$, $\Delta J_z(t_f)$, $\langle J_y(t_f)\rangle$, $\Delta J_y(0)$, and $\langle J_z(0)\rangle$ refer to the new states to be considered and the subscript R denotes that this is the relevant squeezing parameter for the particular form of the Ramsey method of spectroscopy considered. The goal of the paper is to examine ways to make ξ_R less than 1 and as small as possible.

More generally, consider a state with arbitrary $\langle\mathbf{J}\rangle$. Let $\hat{\epsilon}$ denote a direction perpendicular to $\langle\mathbf{J}\rangle$ ($\langle\mathbf{J}\rangle\cdot\hat{\epsilon}=0$) such that $\Delta(\mathbf{J}\cdot\hat{\epsilon})$ is a minimum. This state can always be rotated (by, for example, application of a classical field)

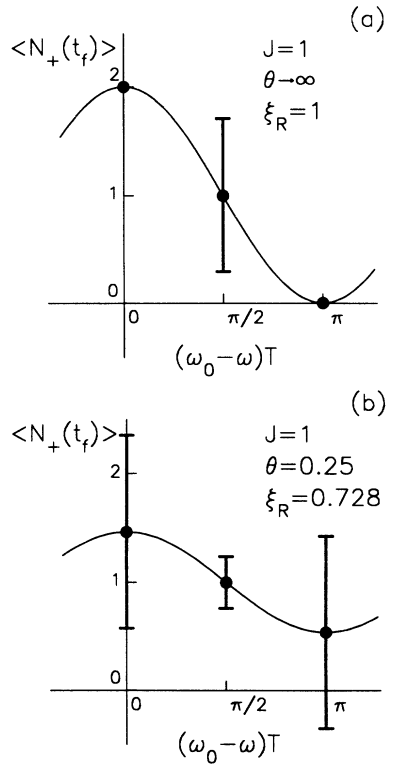

FIG. 5. Plot of $\langle N_+(t_f)\rangle$ and $\Delta N_+(t_f)$ for three values of ω corresponding to $\omega_0-\omega=0$, $\pi/2T$, and π/T, for $N=2$ ($J=1$). For both (a) and (b), $\psi(0)=(e^{-\theta}|1,1\rangle+e^{\theta}|1,-1\rangle)/[2\cosh(2\theta)]^{1/2}$. In (a), we assume $\theta\to\infty$, that is, the initial state is the $|1,-1\rangle$ Dicke state. For $\omega_0-\omega=0$ and π/T, the noise $\Delta N_+(t_f)=0$ since the corresponding final states $\psi(t_f)=|1,1\rangle$ and $|1,-1\rangle$ are eigenstates. However, the sensitivity to frequency fluctuations $\partial\langle N_+(t_f)\rangle/\partial\omega$ also goes to zero at these frequencies, so the signal-to-noise ratio is not improved. In general, for $\psi(0)=|J,-J\rangle$ (or $|J,J\rangle$), the error $\Delta\omega$ in our determination of ω_0 [Eqs. (13) and (22)] is independent of ω. In (b), $\theta=0.25$. This state leads to a reduced value of $\Delta\omega$ for $\omega_0-\omega=\pi/2T$ ($\xi_R=0.728$). However, for $|\omega_0-\omega|\simeq0$ and π/T, $\Delta\omega$ increases substantially over case (a).

so that $\hat{\epsilon}$ and $\langle \mathbf{J} \rangle$ point along the $\hat{\mathbf{y}}$ and negative $\hat{\mathbf{z}}$ axes, respectively. This state can then be used in Ramsey spectroscopy with ξ_R given by Eq. (30). If we define $\Delta J_\perp \equiv \Delta(\mathbf{J}\cdot\hat{\epsilon})$, a more general definition of ξ_R is given by

$$\xi_R = (2J)^{1/2}\Delta J_\perp / |\langle \mathbf{J} \rangle| \ . \tag{31}$$

B. Squeezing parameter to indicate sensitivity to rotation

We may view the squeezing parameter ξ_R as having a more general geometrical interpretation which indicates the degree to which we can sense rotations of angular momentum states. This generalization can then be applied to specific cases such as interferometry [29] or spectroscopy [38]. To see this, first consider a state which has $\langle \mathbf{J} \rangle = -\hat{\mathbf{z}}|\langle J_z \rangle|$ (Fig. 3). Suppose we are interested in measuring a small rotation of $\mathbf{J}$ about the x axis by the angle θ. A way to do this is to measure J_y. We define θ through the relation $\langle J_y \rangle = \sin\theta |\langle \mathbf{J} \rangle|$. The mean-squared noise in θ is given by $(\Delta\theta)^2 = (\Delta J_y)^2 / (\partial \langle J_y \rangle / \partial\theta)^2$. Therefore the precision of the angle measurement is given by $\Delta\theta = \Delta J_y / (\cos\theta |\langle \mathbf{J} \rangle|)$, which is minimized for $\theta = \pm n\pi$ ($n = 0, 1, 2, \ldots$). More generally, for a state with arbitrary $\langle \mathbf{J} \rangle$, consider rotations $\phi(\hat{\eta})$ of $\langle \mathbf{J} \rangle$ about an axis $\hat{\eta}$ where $\langle \mathbf{J} \rangle \cdot \hat{\eta} = 0$. We can measure these rotations by measuring $J_\perp \equiv \hat{\alpha}\cdot\mathbf{J}$ where $\hat{\alpha}\cdot\langle \mathbf{J} \rangle = \hat{\alpha}\cdot\hat{\eta} = 0$. In this case the uncertainty in our measurement of $\phi(\hat{\eta})$ is given by

$$\Delta\phi = \Delta J_\perp / |\langle \mathbf{J} \rangle| \ . \tag{32}$$

If we compare this angle uncertainty to the value $\Delta\phi_{\mathrm{DS}}$ obtained using the Bloch states (states obtained from the $|J, -J\rangle$ Dicke states by a rotation [48]), we can define a squeezing parameter indicating sensitivity to rotation as $\Delta\phi / \Delta\phi_{\mathrm{DS}}$. We have

$$\Delta\phi / \Delta\phi_{\mathrm{DS}} \equiv (2J)^{1/2}\Delta J_\perp / |\langle \mathbf{J} \rangle| = \xi_R \ . \tag{33}$$

Therefore the subscript R can also be used to signify rotation and ξ_R the improved sensitivity to rotations using squeezed-spin states.

From this definition of squeezing, we gain a pictorial representation of what is desired in this kind of squeezed-spin state. Referring to Fig. 3 and Eq. (30), (31), or (33), we desire a state where $|\langle \mathbf{J} \rangle|$ is as long as possible and the error spheroid is compressed as much as possible in a direction perpendicular to $\langle \mathbf{J} \rangle$ [along $\hat{\mathbf{y}}$ in Fig. 3(a)], but, at the same time, minimizing $\Delta J_\perp / |\langle \mathbf{J} \rangle|$. As discussed in Sec. V C and in Refs. [30] and [34], some states show the best squeezing when $|\langle \mathbf{J} \rangle| \to 0$. The pictorial representation of such a state is a spheroid nearly centered on the origin with $\Delta J_y(0) \ll \Delta J_x(0), \Delta J_z(0)$.

C. A simple example (squeezed states for $N = 2$)

Consider two particles which are initially prepared in the state

$$\psi(0) = [2\cosh(2\theta)]^{-1/2} \times (e^{-\theta}|+\rangle_1|+\rangle_2 + e^{\theta}|-\rangle_1|-\rangle_2) \ . \tag{34}$$

This is a correlated or entangled state of particles 1 and 2 since the wave function cannot be written as a direct product (except for $\theta \to \pm\infty$). Many properties of this kind of state have been considered by Rashid [25], who investigated states of the form

$$\Psi'(J, M, \theta) = C_N \exp(-\theta J_z)\exp(-i\pi J_x/2)|J, M\rangle ,$$

where C_N is a normalization constant. The state in Eq. (34) is, to an overall phase factor, the Rashid state $\Psi'(1, 0, \theta)$. It has also been considered in Ref. [32] in the context of the radiation emitted by the two particles. It would be produced by coupling the two particles to a broadband squeezed vacuum [33]. This state has the properties that $\langle J_x(0) \rangle = \langle J_y(0) \rangle = 0$, $\langle J_z(0) \rangle = -\tanh 2\theta$, $\Delta J_x^2(0) = \frac{1}{2}(1 + \mathrm{sech} 2\theta)$, $\Delta J_y^2(0) = \frac{1}{2}(1 - \mathrm{sech} 2\theta)$, $\Delta J_z(0) = \mathrm{sech} 2\theta$, and $\xi_R = \mathrm{sech}\theta[(\cosh 2\theta)/2]^{1/2}$. This state also satisfies the condition $\Delta J_x(0)\Delta J_y(0) = \frac{1}{2}|\langle J_z(0) \rangle|$ and is therefore a minimum-uncertainty state [25]. When θ is large, $\psi(0) \simeq |1, -1\rangle$ and $\xi_R \simeq 1$; this is just the initial state considered in the example in Sec. IV. When θ is small, $\xi_R \simeq (1 + \theta^2/2)/2^{1/2}$. Therefore, as $\theta \to 0$, $\xi_R \to 1/\sqrt{2} = 1/\sqrt{N}$. We can also show that, for $J = 1$, the state of Eq. (34) is the state which minimizes ξ_R.

In Fig. 5, we plot the Ramsey resonance curve ($\langle N_+(t_f) \rangle$ vs ω) when using this initial state for two cases, $\theta \to \infty$ ($\xi_R = 1$) and $\theta = 0.25$ ($\xi_R = 0.728$). We also plot the fluctuations $\Delta N_+(t_f)$ for values of ω given by $(\omega_0 - \omega)T = 0$, $\pi/2$, and π. For $(\omega_0 - \omega)T = 0$ and π, we see that plotting $\Delta N_+(t_f)$ is some what misleading because, for example, values of $N_+(t_f)$ outside the range of 0–2 are not allowed. However, at the primary values of interest, $(\omega_0 - \omega)T = \pm\pi/2$, $\Delta N_+(t_f)$ gives a reasonable representation of the fluctuations between measurements.

From Fig. 5(b), the key point is that, although the amplitude of the Ramsey curve becomes smaller, the noise at the probe frequencies $(\omega_0 - \omega)T = \pm\pi/2$ becomes smaller more rapidly. Therefore the signal-to-noise ratio ($\propto |\Delta\omega|^{-1}$) is increased at these frequencies. It is also clear that the signal-to-noise ratio approaches 0 near the peaks and valleys of the curve; hence it is important to probe near the half-intensity points.

A physical explanation for the noise reduction is as follows. In the Schrödinger picture, for $\theta \to 0$, the final wave function (to an overall phase factor) is given from Eqs. (24) and (34) as

$$\psi(t_f) \simeq |1, 0\rangle = (|+\rangle_1|-\rangle_2 + |-\rangle_1|+\rangle_2)/\sqrt{2} \ .$$

This state has the property that, if J_z is measured for either particle 1 or 2, we find $\langle J_z \rangle = 0$; that is, it is equally likely to find the particle in the $|+\rangle$ or the $|-\rangle$ state. On the other hand, when we measure J_z sequentially for each particle, we find opposite values of J_z for each particle. For example, if when measuring particle 1 we find it to be in the $|+\rangle_1$ state, then $\psi(t_f)$ has been projected into the $|+\rangle_1|-\rangle_2$ state. Therefore, when J_z is measured for particle 2, we find it to be in the $|-\rangle_2$ state. This property of correlated states is at the heart of the correlations observed in two-particle EPR experiments

[1,23]. The correlations exist even if the particles do not interact.

Letting $\theta \to 0$ in Eq. (34) clearly shows the correlations between particles but gives rise to practical problems since the signal ($\propto |\langle J_z(0)\rangle| = \tanh 2\theta$) also approaches 0. More generally, for $\theta \to 0$, $\langle \mathbf{J} \rangle \to 0$ and the signal goes to zero for any form of the (classical) resonance radiation, since any excitation, Ramsey or otherwise, is equivalent to a rotation. Therefore, for example, in the presence of added noise, we want to choose a value of θ which minimizes $|\Delta\omega|$ given by Eq. (21).

D. Squeezed states for other values of N

We first consider $N=1$ ($J=\frac{1}{2}$). We would not expect a way to make $\xi_R < 1$ because there is only one particle and the issue of correlations does not arise. For $J=\frac{1}{2}$, the most general initial pure state can be written in the form

$$\psi(0) = \cos\theta/2 e^{-i\phi/2}|+\rangle + \sin\theta/2 e^{i\phi/2}|-\rangle$$

in which case $\xi_R = (1+\tan^2\theta\cos^2\phi)^{1/2} \geq 1$.

For $N>2$, states which give rise to minimum values of ξ_R are not immediately apparent. For example, for $N=3$, as the parameters of the wave function are varied, local minima can be found. Using a minimization program we find locally minimum states

$$\psi(0) \simeq 0.935|\tfrac{3}{2},\tfrac{3}{2}\rangle + 0.354|\tfrac{3}{2},-\tfrac{1}{2}\rangle$$

and $\psi(0) = \Psi'(\frac{3}{2},\frac{1}{2},0)$, the Rashid state for $\theta \to 0$. These states give locally minimum values of ξ_R with values $\xi_R \simeq 0.76$ and 0.66, respectively. Neither of these states has $\xi_R = 1/\sqrt{N} = 0.577$.

Finding states which minimize ξ_R becomes more complicated for larger N. Nevertheless, we can guess at states which approximate $\xi_R = 1/\sqrt{N}$. When N is odd, consider the relatively simple *final* states (considered previously by Yurke [30] for interferometers)

$$\psi(t_f) = \frac{1}{\sqrt{2}}(|J,\tfrac{1}{2}\rangle + |J,-\tfrac{1}{2}\rangle) \quad (N \text{ odd}) . \tag{35}$$

The appropriate initial states can be obtained through rotations (for example for reversing the order of the Ramsey pulses). These states have the property that $\xi_R = (1/\sqrt{N})[2/(1+1/N)]$. When N is even consider the *final* states

$$\psi(t_f) = \frac{1}{\sqrt{2}}\sin\alpha|J,1\rangle + i\cos\alpha|J,0\rangle - \frac{1}{\sqrt{2}}\sin\alpha|J,-1\rangle \quad (N \text{ even}) . \tag{36}$$

For these states, $\xi_R = (1+N/2)^{-1/2}/\cos\alpha$. For $N=2$, this state is equivalent to the Rashid state of Eq. (34). We see that ξ_R is minimized for $\alpha \to 0$, but as noted in Sec. V C, the amplitude of the Ramsey curve also goes to zero as $\alpha \to 0$. Agarwal and Puri [34] have shown that the states of Rashid [25]

$$\Psi'(J,M,\theta) = C_N \exp(-\theta J_z)\exp(-i\pi J_x/2)|J,M\rangle$$

can be used in Ramsey spectroscopy and give minimum values of $\xi_R = [1+(J^2-M^2)/J]^{-1/2}$ for $\theta \to 0$. Therefore, for N even, $\xi_R = (1+N/2)^{-1/2}$ with $M=0$. For N odd, $\xi_R = [1+(N^2-1)/2N]^{-1/2}$ with $M = \pm\frac{1}{2}$. This gives a value of ξ_R somewhat smaller than the states of Eq. (35).

E. Minimum value of ξ_R

Although the particular Rashid states considered by Agarwal and Puri [34] give the best value of squeezing of the states considered above, it is useful to consider the minimum possible value of ξ_R. We find that $\xi_R \geq N^{-1/2}$ from the inequalities

$$\xi_R = (2J)^{1/2}\Delta J_y/|\langle J_z\rangle| \geq (J/2)^{1/2}/\Delta J_x \geq (2J)^{-1/2} = N^{-1/2} . \tag{37}$$

The first inequality follows from the uncertainty principle applied to angular momentum, $\Delta J_y \geq |\langle J_z\rangle|/2\Delta J_x$ (see Sec. VI A). The second inequality follows from $\Delta J_x \leq J$. This last relation can be seen by noting that, if we quantize the angular momentum along the x direction, it is straightforward to show that the states with the largest value of ΔJ_x are of the form

$$\psi_x = 2^{-1/2}(|J,J\rangle_x + e^{i\phi}|J,-J\rangle_x) ,$$

in which case $\Delta J_x = J$. In the states considered above, the only state which shows this maximum degree of squeezing is the $J=1$ state considered in Eq. (34).

VI. ALTERNATE DEFINITIONS OF SPIN SQUEEZING

A. Squeezing parameter based on angular-momentum commutation relations

Different definitions of spin squeezing can be used depending on the context in which squeezing is considered. From the commutation relations for angular momentum, the uncertainty relations between different components of the angular momentum are given by

$$\Delta J_x \Delta J_y \geq |\langle J_z\rangle/2| \tag{38}$$

and the expressions which follow from cyclic permutations of indices. From these uncertainty relations, it is natural to define squeezed-spin states as states where $\Delta^2 J_i < |\langle J_j\rangle/2|$ for $i \neq j$. Hence a squeezing parameter for this "natural" definition of squeezing might be written as

$$\xi_n = \Delta J_i/|\langle J_j\rangle/2|^{1/2}, \quad i \neq j \in (x,y,z) . \tag{39}$$

Squeezing in the context of this definition is discussed in Refs. [26–28] and [33]. For example, Walls and Zoller [26] illustrate the relation between spin squeezing defined in this way and the squeezing in resonance fluorescence light from two-level atoms. This squeezing is exhibited by Bloch states which are states derived from the $|J,-J\rangle$ Dicke states by a rotation. We can see this using Eq. (10). During the first Ramsey pulse where $\boldsymbol{\omega}' \simeq \omega_1 \hat{\mathbf{y}}$ (corresponding to a rotation about $\hat{\mathbf{y}}$), the angular-momentum operators transform according to

$$J_z(t)=J_z(0)\cos\omega_1 t - J_x(0)\sin\omega_1 t$$

and

$$J_x(t)=J_x(0)\cos\omega_1 t + J_z(0)\sin\omega_1 t \ .$$

Therefore, if we define squeezing as $\xi_n \equiv \Delta J_x / |\langle J_z \rangle/2|^{1/2}$, we find $\xi_n(t)=\cos^{1/2}\omega_1 t \leq 1$ when $\psi(0)=|J,-J\rangle$.

B. Squeezing parameter to indicate the degree of correlation

As pointed out by Kitagawa and Ueda [36] the definition of squeezing discussed in Sec. VI A does not necessarily reflect the correlations between particles. For example, the Bloch states remain uncorrelated under rotation [cf. Eq. (28)] even though they show $\xi_n < 1$. Kitagawa and Ueda therefore regard the spin to be squeezed only if the variance of one spin component $J_\perp$ normal to the mean spin vector is smaller than the variance for a Bloch state ($=J/2$) [36]. In this view, a spin-squeezing parameter might be defined as

$$\xi_S = \Delta J_\perp / (J/2)^{1/2} \ , \tag{40}$$

where the $\perp$ subscript refers to an axis perpendicular to $\langle \mathbf{J} \rangle$ where the minimum value of ΔJ is obtained. A squeezed-spin state ($\xi_S < 1$) can be rotated so that $\langle \mathbf{J} \rangle = \langle J_z \rangle \hat{\mathbf{z}}$ and $\Delta J_\perp = \Delta J_y$ and could be used in Ramsey spectroscopy (or interferometry) with $\xi_R = (J/|\langle J_z \rangle|)\xi_S$. In Ref. [38], we used a somewhat different definition of ξ_S which we called ξ_{spin}.

VII. GENERATION OF SQUEEZED-SPIN STATES

As discussed in the last section, states for which $\xi_n < 1$ can be generated by rotations of the $|J,\pm J\rangle$ Dicke states. Since $\xi_R = \xi_S = 1$ for these states, we do not consider them further. The specific correlated or squeezed states considered in Refs. [29–31] and in Eqs. (35) and (36) above were constructed to emphasize the benefits of spin squeezing in the context of various experiments, but generators for these states were not given.

Rashid [25] investigated the class of angular-momentum states which satisfy the equality in Eq. (38). These minimum-uncertainty or "intelligent" states can be formed from the $|J,M\rangle$ Dicke states by the transformation of the form

$$\Psi'(J,M,\theta) = C_N \exp(-\theta J_z)\exp(-i\pi J_x/2)|J,M\rangle \ ,$$

where C_N is a normalization constant. These kinds of states show $\xi_R \simeq N^{-1/2}$ for $\theta \to 0$ as discussed in Sec. V D. Agarwal and Puri have shown [33] that the $\Psi'(J,0,\theta)$ Rashid states for integral J can be created by the interaction of an ensemble of two-level or spin-$\frac{1}{2}$ particles with broadband squeezed vacuum radiation.

Barnett and Dupertuis [32] considered the correlated states between pairs of particles (1 and 2) generated by a Hamiltonian of the form $H = i(g^* J_{1+} J_{2+} - g J_{1-} J_{2-})$, where $J_+ = J_x + iJ_y$ and $J_- = J_x - iJ_y$ are the usual raising and lowering operators. Kitagawa and Ueda [35,36] considered the squeezed-spin states, for arbitrary N, generated by interaction of the spins through nonlinear Hamiltonians of the form $H = \hbar\chi J_z^2$ and $H = \hbar\chi(J_+^2 - J_-^2)/2i$. Both of these interactions lead to useful squeezing. They have shown that the Coulomb interaction between electrons in the two arms of an electron interferometer corresponds to a Hamiltonian of the form $H = \hbar\chi J_z^2$ and might be used to generate the squeezed states in that system.

A. Coupling to a harmonic oscillator

In Ref. [38], we considered the spin squeezing produced when an ensemble of two-level particles was coupled to a (single) harmonic oscillator. One reason we considered this coupling was the prior theoretical demonstration of the complementary effect—harmonic-oscillator squeezing through the same coupling to two-level systems [57] (see also Ref. [21]). The hope was that, for certain initial conditions, the same type of system might produce spin squeezing. As discussed below, it may be possible to realize coupling to a suitable harmonic oscillator, whereas we have not thought of a practical way to realize the couplings discussed by Kitagawa and Ueda [35,36] for ensembles of two-level atoms.

Therefore, in the laboratory frame, the Hamiltonian we consider is given by

$$\begin{aligned} H &= \hbar\omega_0 J_z + \hbar\omega_z (a^\dagger a + \tfrac{1}{2}) + H_I \ , \\ H_I &= -2\hbar\Omega(a^\dagger + a)(J_+ + J_-)\cos\omega_m t \ , \end{aligned} \tag{41}$$

where the first term is given by Eqs. (2) and (5), $a^\dagger$ and a are the creation and annihilation operators for the harmonic oscillator of frequency ω_z and amplitude $z = z_0(a + a^\dagger)$, and Ω represents the strength of the coupling, which we assume, in general, is sinusoidally modulated at frequency ω_m. It will be useful to transform to the interaction picture where, for $\Omega = 0$, the operators (or wave functions) are constant in time. In this interaction picture, the new operators are given by $\tilde{a} = a\exp(i\omega_z t)$, $\tilde{J}_- = J_-\exp(i\omega_0 t)$, and the adjoint expressions. The operators $\tilde{J}$ are the operators in the rotating frame introduced in the subsection of Sec. II. In this interaction picture, the Hamiltonian representing the coupling becomes

$$\begin{aligned} H_I = -2\hbar\Omega\cos\omega_m t [& a^\dagger J_+ e^{i(\omega_z+\omega_0)t} + a J_- e^{-i(\omega_z+\omega_0)t} \\ & + a^\dagger J_- e^{i(\omega_z-\omega_0)t} \\ & + a J_+ e^{i(\omega_0-\omega_z)t}] \ , \end{aligned} \tag{42}$$

where, for convenience, we have dropped the tilde symbols ($\sim$). Resonant interactions occur for two values of ω_m. For $\omega_z \neq \omega_0$ and $\omega_m = \pm(\omega_0 - \omega_z)$, the Hamiltonian is

$$H_1 = -\hbar\Omega(a J_+ + a^\dagger J_-) \ , \tag{43}$$

plus high-frequency terms which we neglect (rotating-wave approximation). This is the Hamiltonian of the Jaynes-Cummings model [58] which is of considerable interest in quantum optics. For $\omega_z \neq \omega_0$ and $\omega_m = \pm(\omega_0 + \omega_z)$, the Hamiltonian is

$$H_2=-\hbar\Omega(a^\dagger J_+ + aJ_-)\ , \tag{44}$$

plus high-frequency terms which we neglect. When $\omega_0=\omega_z$, Ω should be replaced by 2Ω in the expressions for H_1 and H_2. For brevity, we will assume $\omega_z\neq\omega_0$. H_1 and H_2 are essentially equivalent since H_1 becomes H_2 if we switch the roles of the $|+\frac{1}{2}\rangle$ and $|-\frac{1}{2}\rangle$ states for each particle.

We now consider the preparation of the spins into correlated states through the interactions H_1 or H_2. The states which are prepared this way could then be used in Ramsey spectroscopy. For simplicity of notation, we will consider this preparation phase to start at $t=0$. However, this time should not be confused with the time when the first Ramsey pulse is applied.

B. Approximate solution

One way squeezing can be imparted to the spins is by first squeezing the harmonic oscillator and transferring this squeezing to the spins through H_1 [38]. To get a feeling for how this works without making the problem mathematically complicated, consider the following special case. The spin is assumed to be initially prepared in the $|J,-J\rangle$ Dicke state and the harmonic oscillator is prepared in a squeezed vacuum state characterized by $\langle z(t=0)\rangle=\langle\dot{z}(0)\rangle=0$ and $\Delta z(0)<\Delta z(\text{coherent state})=z_0$. We can characterize the squeezing of the harmonic oscillator by the parameters $\xi_z(t)\equiv\Delta z(t)/z_0$ or $\xi_v(t)\equiv\Delta\dot{z}(t)/(\omega_z z_0)$. The condition $\xi_z<1$ indicates amplitude squeezing and $\xi_v<1$ indicates velocity or momentum squeezing. When H_1 applies, the Heisenberg equations of motion are

$$da/dt=i\Omega J_-,\quad dJ_-/dt=-2i\Omega a J_z\ , \tag{45}$$

and the adjoint expressions. We now make the assumption that the initial mean number of quanta $\langle n(0)\rangle\equiv\langle a^\dagger(0)a(0)\rangle$ in the harmonic oscillator is small enough and/or N is large enough that the value of $\langle J_z\rangle$ does not change appreciably during the time H_1 is applied. In this case, we make the approximation $J_z(t)=-JI$, where I is the identity operator. With this approximation, the Heisenberg equations of motion can be solved analytically to give

$$J_-(t)=J_-(0)\cos\Omega_N t+iN(\Omega/\Omega_N)a(0)\sin\Omega_N t\ , \tag{46}$$

$$a(t)=a(0)\cos\Omega_N t+iJ_-(0)N^{-1/2}\sin\Omega_N t\ , \tag{47}$$

and the adjoint expressions, where $\Omega_N^2\equiv N\Omega^2$. From these equations, we find

$$\xi_R^2(t)=\xi_S^2(t)=\cos^2\Omega_N t+\xi_z^2(0)\sin^2\Omega_N t\ , \tag{48}$$

$$\xi_{R,x}^2(t)=\cos^2\Omega_N t+\xi_v^2(0)\sin^2\Omega_N t\ , \tag{49}$$

$$\xi_z^2(t)=\xi_z^2(0)\cos^2\Omega_N t+\sin^2\Omega_N t\ , \tag{50}$$

and

$$\xi_v^2(t)=\xi_v^2(0)\cos^2\Omega_N t+\sin^2\Omega_N t\ . \tag{51}$$

In Eq. (49), we make the definition $\xi_{R,x}\equiv(2J)^{1/2}\Delta J_x/|\langle J_z\rangle|$. If a state with $\xi_{R,x}<1$ is produced, it could be used in Ramsey spectroscopy by first rotating the state by $\pi/2$ about the z axis so that $\xi_{R,x}\rightarrow\xi_{R,y}\equiv\xi_R$. From Eqs. (48) and (49), we can create squeezed-spin states by first squeezing the harmonic oscillator ($\xi_z(0)<1$ or $\xi_v(0)<1$) and transferring the squeezing to the spins. Correspondingly, from Eqs. (50) and (51) we see that the squeezing is "drained away" from the harmonic oscillators as it is transferred to the spins. In this small-angle approximation, squeezing is transferred to the spins like wave-function exchange between harmonic oscillators [18]. The squeezing is sinusoidally transferred back and forth between the harmonic oscillator and the spins; however, in a more precise treatment, where we no longer assume $\langle J_z\rangle$ to be constant, this will no longer be true. We find the same expressions for $\xi_R(t)$, $\xi_{R,x}(t)$, $\xi_z(t)$, and $\xi_v(t)$ when $\omega_m=\pm(\omega_0+\omega_z)$ (H_2 applies), $\psi(0)=|J,+J\rangle$, and if we make the small-angle approximation $J_z=+JI$.

For H_1, if we instead assume $\psi(0)=|J,+J\rangle$ and make the small-angle approximation $J_z(t)=+JI$, we find

$$\xi_R^2(t)=1+[\xi_z^2(0)+1]\sinh^2\Omega_N t\ , \tag{52}$$

$$\xi_{R,x}^2(t)=1+[\xi_v^2(0)+1]\sinh^2\Omega_N t\ , \tag{53}$$

$$\xi_z^2(t)=\xi_z^2(0)+[1+\xi_z^2(0)]\sinh^2\Omega_N t\ , \tag{54}$$

$$\xi_v^2(0)=\xi_v^2(0)+[1+\xi_v^2(0)]\sinh^2\Omega_N t\ . \tag{55}$$

The same expressions are found for H_2 if we assume $\psi(0)=|J,-J\rangle$ and make the small-angle approximation $J_z(t)=-JI$. In these cases, for short times, no squeezing is transferred to the spins and the harmonic-oscillator squeezing degrades.

C. Numerical solution

Because of the limited validity of the small-angle approximation, we have integrated Schrödinger's equation for H_1 and H_2 for some special cases. We write the wave function for the combined harmonic-oscillator–spin ensemble as

$$\Psi_c(t)=\sum_{n,M}C_{n,M}(t)|n\rangle|M\rangle\ , \tag{56}$$

where $|n\rangle$ are the harmonic-oscillator eigenstates and we use the shorthand notation $|M\rangle=|J,M\rangle$ since J is a constant of the motion for H_1 and H_2. From Schrödinger's equation, we find for H_1

$$dC_{n,M}/dx=i(n+1)^{1/2}[j(j+1)-M(M-1)]^{1/2}C_{n+1,M-1}+in^{1/2}[j(j+1)-M(M+1)]^{1/2}C_{n-1,M+1}\ , \tag{57}$$

where $x\equiv\Omega t$. We have integrated this equation and the corresponding one for H_2 using a fourth-order Runge-Kutta method [59]. For the initial wave function, we assume the atoms and harmonic oscillator are uncorrelated so that the wave function can be written as a direct product

$$\Psi_c(0)=\left[\sum_n c_n(0)|n\rangle\right]\psi(0)\ , \tag{58}$$

where $c_n(0)$ are the initial harmonic-oscillator wave-function coefficients [60] and we will assume $\psi(0)=|J,-J\rangle$ or $|J,+J\rangle$. Of course, we must truncate the basis of harmonic-oscillator states; an adequate number of states is determined by increasing the basis until the result remains unchanged.

For $J=1$, we also solved Schrödinger's equation for H_1 and H_2 with a different numerical approach. For $J=1$, the Hamiltonians H_1 or H_2 can be written as blocks of 3×3 matrices on the diagonal and zeros elsewhere. Explicitly, H_1 only couples states where $n+M$ is a constant and H_2 only couples the states $|n-1\rangle|-1\rangle$, $|n\rangle|0\rangle$, and $|n+1\rangle|+1\rangle$. The 3×3 matrices corresponding to the Hamiltonian of the coupled states were diagonalized and the wave function for the combined harmonic-oscillator–spin ensemble written as a sum over the eigenstates. The time evolution of the wave function

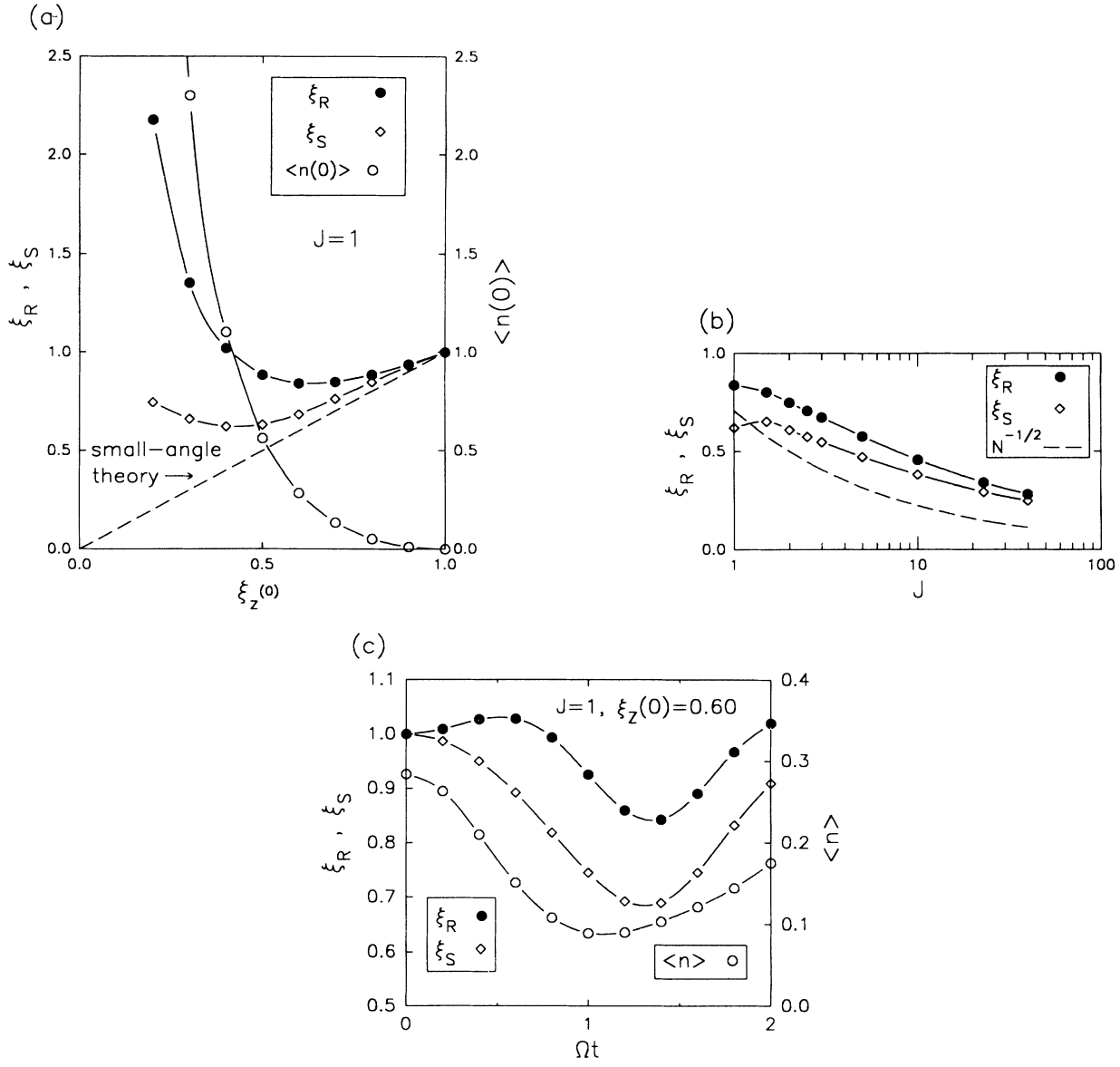

FIG. 6. Plots of ξ_R [Eq. (30)] and ξ_S [Eq. (40)] assuming the squeezed-spin states are prepared by coupling a single harmonic oscillator to the spins via the interaction H_1 [Eq. (43)]. We assume $\psi(0)=|J,-J\rangle$ and the harmonic oscillator to be initially prepared in the squeezed vacuum state where $\langle z(0)\rangle=\langle\dot{z}(0)\rangle=0$ and $\xi_z(0)<1$. In (a), $J=1$. We plot the values of the first minima of ξ_R and ξ_S as a function of time after H_1 is turned on [refer to (c)] vs the initial value of $\xi_z(0)$. We also plot the value of $\langle n(0)\rangle\equiv\langle a^\dagger a\rangle$ vs $\xi_z(0)$. In addition, we plot the prediction of the small-angle theory, $\xi_R=\xi_S=\xi_z(0)$, as a dashed line. As expected, the small-angle theory is valid only for very small values of $\xi_z(0)$ (or $\langle n\rangle$). In (b), we plot the first minimum values of ξ_R and ξ_S less than 1, after H_1 is turned on, vs J. For each point, $\xi_z(0)$ has been adjusted to give the smallest value of ξ_R and ξ_S. In (c), we plot ξ_R, ξ_S, and $\langle n\rangle$ as a function of time for $J=1$, and $\xi_z(0)=0.60$. At $\Omega t\simeq1.35$, ξ_R reaches its minimum value of $\simeq0.84$.

is then obtained from the time evolution of the eigenstates. With this method a larger number of harmonic-oscillator states could be included in the calculation. We obtained results that agreed with the numerical approach described above. This method can be generalized for $J>1$ with the complication that $(2J+1)\times(2J+1)$ matrices would need to be diagonalized.

In Fig. 6, we plot ξ_R and ξ_S for H_1 assuming $\psi(0)=|J,-J\rangle$ and assuming the oscillator is initially in an amplitude-squeezed vacuum state where $\langle z(0)\rangle = \langle \dot{z}(0)\rangle = 0$ and $\xi_z(0)<1$. This figure indicates the limited validity of the small-angle approximation, which is shown as a dashed line. We see that there are states for which $\xi_s<1$ while $\xi_R>1$. This emphasizes the need to define squeezing in the context of a particular problem. From Fig. 6(a), we also see that the minimum values of ξ_S and ξ_R are obtained for different initial values of $\xi_z(0)$. In Fig. 6(c) we plot the evolution of ξ_R, ξ_S, and $\langle n\rangle$ as functions of time for $J=1$ and $\xi_z(0)=0.60$. Initially, ξ_R becomes greater than 1 but eventually reaches a minimum value of 0.840 corresponding to that shown in Fig. 6(a).

In Fig. 7, we plot $\xi_{R,x}$ and ξ_S for H_2 assuming $\psi(0)=|J,-J\rangle$ and assuming the oscillator is initially in a coherent state where $\langle z(0)\rangle\neq 0$, $\langle \dot{z}(0)\rangle = 0$, and $\xi_z(0) = \xi_v(0) = 1$. Before using the resulting states in Ramsey spectroscopy, we want to first rotate $\langle \mathbf{J}\rangle$ so that it points along the negative z axis and then rotate the state about the z axis by $\pi/2$ so that the squeezing in the x direction is transferred to the y direction ($\xi_{R,x}\rightarrow\xi_{R,y}\equiv\xi_R$). The harmonic oscillator, in combination with H_2, drives the spin $\langle \mathbf{J}\rangle$ to lie in the y-z plane. This is indicated in Fig. 7(c) where we plot, for $J=1$, $\xi_{R,x}$, $\xi_{S,x}$, and $\langle n\rangle$ vs time and $\langle \mathbf{J}(t)\rangle$ as viewed in the $-\hat{\mathbf{x}}$ direction, assuming the value of $\langle n(0)\rangle$ which minimizes $\xi_{R,x}$. Spin squeezing along these lines may be of practical interest since we require the initial harmonic-oscillator state to be only a coherent state, not a squeezed state.

A squeezed state of the harmonic oscillator can be generated by parametric pumping of the oscillator at frequency $2\omega_z$. In the laboratory frame this pumping interaction can be represented by

$$H_P(\text{lab}) = -2\hbar\Omega_P(a+a^\dagger)^2\sin 2\omega_z t \propto z^2\sin 2\omega_z t \ .$$

If we add this interaction to H_1, the total Hamiltonian in the interaction frame becomes

$$H_3 = -\hbar\Omega(aJ_+ + a^\dagger J_-) + i\hbar\Omega_P(a^2-(a^\dagger)^2) \ , \qquad (59)$$

plus high-frequency terms which we neglect. In general, we could let Ω_P vary in time. The case considered in Fig. 6 is equivalent to having Ω_P nonzero and large for a very short time after $t=0$ and then allowing the system to evolve under the influence of H_1. In Fig. 8, we consider a special case where Ω_P and Ω are constant in time and applied together. We show a plot of ξ_R and ξ_S vs time for $J=1$, $\psi(0)=|1,-1\rangle$, the harmonic oscillator initially in the vacuum state [$\langle z(0)\rangle = \langle \dot{z}(0)\rangle = 0$, and $\xi_z(0)=\xi_v(0)=1$], and $\Omega_P/\Omega = 0.23$. This value of Ω_P/Ω yields a (local) minimum in ξ_R for these initial conditions.

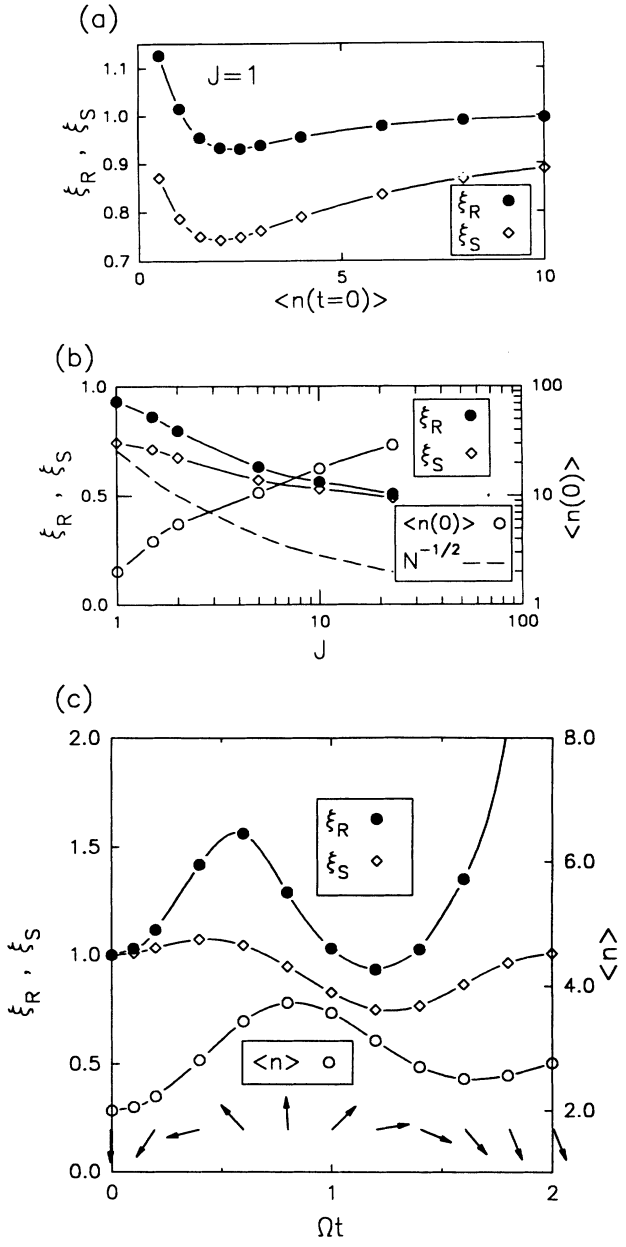

FIG. 7. Plots of $\xi_{R,x}$ [or ξ_R, Eq. (31)] and ξ_S [Eq. (40)] assuming the squeezed-spin states are prepared by coupling a harmonic oscillator to the spins via the interaction H_2 [Eq. (44)]. We assume $\psi(0)=|J,-J\rangle$ and the harmonic oscillator is initially prepared in a coherent state where $\langle z(0)\rangle\neq 0$, $\langle \dot{z}(0)\rangle = 0$, and $\xi_z(0)=\xi_v(0)=1$. In (a), $J=1$. We plot the values of the first minima of ξ_R and ξ_S, as a function of time after H_2 is turned on [refer to (c)] vs $\langle n(0)\rangle$. In (b), we plot the values of the first minima of ξ_R and ξ_S less than 1 after H_2 is turned on vs J. For each point, $\langle z(0)\rangle$ has been adjusted to give the smallest value of ξ_R and ξ_S. The harmonic oscillator, in combination with H_2, drives the spin $\langle \mathbf{J}\rangle$ to lie in the y-z plane. Before using the resulting states in Ramsey spectroscopy, we want to first rotate $\langle \mathbf{J}\rangle$ so that it points along the negative z axis and then rotate the state about the z axis by $\pi/2$ so that the squeezing in the x direction is transferred to the y direction ($\xi_{R,x}\rightarrow\xi_{R,y}\equiv\xi_R$). In (c), we plot, for $J=1$, $\xi_{R,x}$, $\xi_{S,x}$, and $\langle n\rangle$ vs time and $\langle \mathbf{J}(t)\rangle$, shown as an arrow, as viewed in the $-\hat{\mathbf{x}}$ direction, assuming the value of $\langle n(0)\rangle$ which minimizes $\xi_{R,x}$.

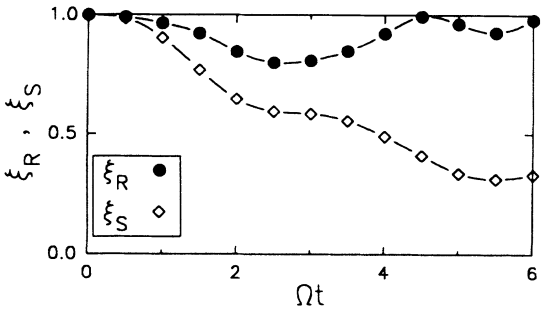

FIG. 8. For $J=1$, we plot ξ_R [Eq. (31)] and ξ_S [Eq. (40)] vs time assuming the squeezed-spin state is prepared by coupling a parametrically pumped harmonic oscillator to the spins via the interaction H_3 [Eq. (59)]. We assume $\psi(0)=|1,-1\rangle$ and the harmonic oscillator is initially prepared in the vacuum state. The curves use the value $\Omega_P/\Omega=0.23$ which minimizes (locally) the value of ξ_R at $\Omega t\simeq 2.5$. At certain times, the values of both ξ_R and ξ_S are reduced below those found in Fig. 6(a).

The values of both ξ_R and ξ_S are less than in the case of Fig. 6(a).

VIII. POSSIBLE EXPERIMENTAL METHODS

As shown by Agarwal and Puri [33,34], a way to produce good squeezing is to couple the spins to a broadband squeezed vacuum. However, this may be difficult in practice, because all spatial modes of the field must be squeezed [61]. These modes are then properly phased only at a particular spatial location and the atoms must all be localized about this point to within a small fraction of a wavelength. For optical transitions with stored ions this is difficult because the Coulomb repulsion typically results in ion-ion separations of more than 1 μm. Neutral atoms could be confined with spacings less than λ, but then the direct dipole-dipole coupling must be included. An alternative strategy might be to confine the atoms in a cavity that is driven by a squeezed vacuum field [61].

From the previous section, another way to produce spin squeezing is to first prepare a harmonic oscillator in a squeezed or coherent state and then couple the oscillator to the spins through a Jaynes-Cummings-type interaction [Eqs. (43) or (44)]. Using the extensive work on "cavity QED" as a guide, this could be accomplished by the interaction of an ensemble of atoms with a suitably prepared electromagnetic field of a single cavity mode [4–7,62–64]. In these types of experiments, the presence of thermal noise and/or cavity and atomic relaxation would reduce the degree of spin squeezing that could be achieved. Although we can expect these problems to be overcome in the future, it may be useful to consider alternate systems. Our experiments have led us to consider coupling of the internal levels of atoms to a different harmonic oscillator—that associated with the oscillation of atoms in a trap. In this paper, we will concentrate on the use of trapped atomic ions, but many of the considerations apply to trapped neutral atoms as well.

A. Trapped-atomic-ion oscillator

The interest in a trapped-ion oscillator is due to its potential immunity from relaxation and thermal noise excitation. To a good approximation, a single ion confined in an ion trap [65,66] can be modeled as a charged harmonic oscillator. For an ensemble of ions localized near the center of the trap this model is also valid for the center-of-mass (c.m.) motion of the ensemble [66]. In what follows, we will assume all internal mode frequencies are shifted away from the c.m. frequency by the ions' Coulomb interaction. The c.m. charged harmonic oscillator is subject to radiative decay and heating from the environment. It can be considered to be confined in a cavity formed by the trap electrodes. Typically, the wavelength of the harmonic-oscillator radiation (corresponding to oscillation frequencies of a few megahertz or less) is much larger than the dimensions of the trap electrodes. A useful representation of this situation is to model the c.m. motion of the harmonically bound ion (in one direction) as a series LC circuit which is shunted by the capacitance of the trap electrodes as shown in Fig. 9 [66]. The resistance r is due to losses in the electrodes and conductors which connect the electrodes. The equivalent inductance of the ions is given [66] by $l\simeq md^2/N(Zq)^2$ where m is the ion mass, d the characteristic internal dimension of the ion-trap electrodes, N the ion number, Zq the charge of a single ion (q=charge of the proton), and we neglect geometrical factors on the order of 1. The resistance r both damps and imparts thermal energy to the ions with time constant l/r. To characterize the damping and thermal heating, we calculate the time t^* for heating the ion's c.m. motion from the $n=0$ to the $n=1$ state,

$$t^*=l\hbar\omega_z/(rk_BT)\simeq 2.9(\omega_z/2\pi)d^2M(u)/(NrTZ^2)\ , \tag{60}$$

where k_B is Boltzmann's constant, T the temperature of

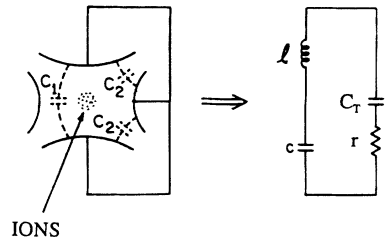

FIG. 9. Equivalent circuit representation of one component (z) of the trapped ions' center-of-mass motion coupled to the surrounding trap electrodes (from Ref. [66]). We have $l\simeq md^2/N(Zq)^2$ where m is the ion mass, d the characteristic internal dimension of the ion-trap electrodes, N the ion number, Zq the charge of a single ion (q=charge of proton), and we neglect geometrical factors on the order of unity. The resistance r is due to losses in the electrodes and conductors which connect the electrodes. The equivalent capacitance of the ion, $c=1/\omega_z^2 l$, is typically much less than C_T which is usually on the order of a few picofarads. As discussed in the text, damping and thermal heating from r can be neglected in many cases.

resistor r, ω_z is the oscillation frequency, and the ion mass M is expressed in atomic mass units. For $\omega_z/2\pi=3$ MHz, $d=2$ mm, $M=100$ u, $N=2$, $r=0.1\Omega$, $T=300$ K, and $Z=1$, we obtain $t^*\simeq 58$ s. In this case, and in general when $\hbar\omega_z \ll k_B T$, the decay time from $n=1$ to $n=0$ is much longer. In the experiment reported in Ref. [13], ($\omega_z/2\pi\simeq 5$ MHz, $d\simeq 0.7$ mm, $M\simeq 200$ u, $N=1$, $T\simeq 300$ K, and $Z=1$), t^* was measured to be 0.17 s even though no care was taken to make r small or to reduce external sources of noise. If we can make Ω large enough ($\gg 1/t^*$), it should be possible to avoid the effects of damping and thermal heating on the ion harmonic oscillator.

Similarly, it should be possible to avoid radiative relaxation in the two-level system. This is particularly true if the levels are separated by rf or microwave frequencies where radiative decay rates can be extremely small [41]. Even at optical frequencies, many forbidden transitions have radiative decay times on the order of seconds or longer and may be viable as candidates for spin squeezing.

B. Squeezed or coherent states of ion motion

A single trapped ion can be laser cooled to its quantum ground state of motion [13]. It should also be possible to extend this technique to cool the c.m. motion of an ensemble of ions to the ground state. In analogy with methods used in quantum optics, a squeezed vacuum state of the c.m. mode (appropriate for Fig. 6) could be obtained from the ground state by suddenly changing the ion's well depth or parametrically modulating the well depth at $2\omega_z$ as indicated by the second term in Eq. (59) [17,18]. A coherent state of nonzero amplitude (appropriate for Fig. 7) could be obtained from the vacuum state by suddenly shifting the center position of the ions' well, or by driving the oscillator with a classical resonant excitation [17,18].

Cirac *et al.* [19] have shown that the ion could be laser cooled and squeezed at the same time by superimposing the nodes of two standing-wave laser beams at the mean position of the ions and tuning the laser frequencies to the first lower and upper sidebands of the two-level transition frequency, that is, to $\omega_0-\omega_z$ and $\omega_0+\omega_z$. Independently of the way the harmonic-oscillator state is produced, the phase of the oscillator and/or squeezing must be referenced to the phase of the clock radiation in a predictable and reproducible way.

C. Possible realizations of the Jaynes-Cummings-model coupling

After the harmonic-oscillator state is prepared, squeezing could be imparted to the spins (or two-level systems) by application of the Jaynes-Cummings interaction given by Eqs. (43) or (44). This form of coupling has already been realized to couple the spin and cyclotron motion of a single electron in the classic g-2 experiments of Dehmelt and his collaborators [67]. In Ref. [38], we considered one possible realization of the Jaynes-Cummings model for atoms. We considered N ions having an unpaired outer electron which are trapped along the axis of a linear rf trap [68] where, here, we take the axis of the trap to be in the y direction. The ions are subjected to a homogeneous magnetic field which quantizes the spins according to Eq. (2). We then superimpose an inhomogeneous field gradient $B'=\partial B_x/\partial z$ whose value, averaged over the ions' orbits, is zero. However, as the ions oscillate, they experience a motional oscillating magnetic field which tends to flip the spin and reduce or increase the ions' c.m. harmonic oscillator as in Eq. (43) for H_1 [69]. The B' field could be generated by a current $I\hat{\mathbf{y}}$ in two wires (which could double as trap electrodes) situated at the positions $z=\pm z_T$ relative to the ions. We find $\Omega/2\pi\simeq 2I_y z_T^{-2}(M\omega_z/2\pi)^{-1/2}$, where I_y, z_T, M, and $\omega_z/2\pi$ are expressed in ampères, centimeters, atomic mass units, and megahertz, respectively. For $I_y=0.1$ A, $z_T=0.01$ cm, $M=24$ u ($^{24}Mg^+$), and $\omega_z/2\pi=1$ MHz, we find $\Omega/2\pi\simeq 400$ Hz.

Blockley, Walls, and Risken [70] have shown that the Jaynes-Cummings model is realized for a harmonically bound atom or ion which interacts with a traveling-wave laser tuned near the transition frequency of the atom. They assume the atom is confined to the Lamb-Dicke limit and the resulting coupling strength is much smaller than the oscillator frequency [$\Omega \ll \omega_z$ in our Eq. (41)]. If the laser is tuned to the first upper or lower motional sideband of the atomic transition, and spontaneous emission from the excited state can be neglected, Rabi oscillations occur between ground and excited states accompanied by oscillations between adjacent harmonic-oscillator states. Cirac *et al.* [71] have shown that the Jaynes-Cummings model is realized for the harmonic motion of a two-level ion confined to the Lamb-Dicke limit whose mean position is located at the node of a standing-wave laser field tuned near the ion's transition frequency. In both cases, if a suitably narrow optical level (one with weak relaxation) can be used, one might hope to impart squeezing to optical levels. These schemes could, in principle, also be applied to transitions of much lower frequency (infrared or microwave frequencies). The coupling Ω would be reduced for the same value of ω_z (reduced Lamb-Dicke parameter) but the radiative decay could be expected to be considerably reduced.

References [72–74] and [18] have theoretically considered the use of stimulated Raman transitions to achieve laser cooling of trapped ions to the zero-point energy. (Stimulated Raman transitions have recently been used to cool free atoms to a kinetic energy less than that corresponding to the recoil of one photon [75].) The systems used to achieve this cooling can also be used to realize the Jaynes-Cummings model. Under certain conditions, stimulated Raman transitions produce a Rabi oscillation [18] which can be described by an effective Jaynes-Cummings interaction. For convenience, we use the notation of Ref. [18].

Reference [18] considered stimulated Raman laser cooling to proceed by repeated applications of a sequential, two-step process. Figure 10 illustrates the first step of this process, where we have restricted our attention to harmonic motion (of frequency ω_z) along one direction taken to be the $\hat{\mathbf{z}}$ direction. The eigenstates of the system

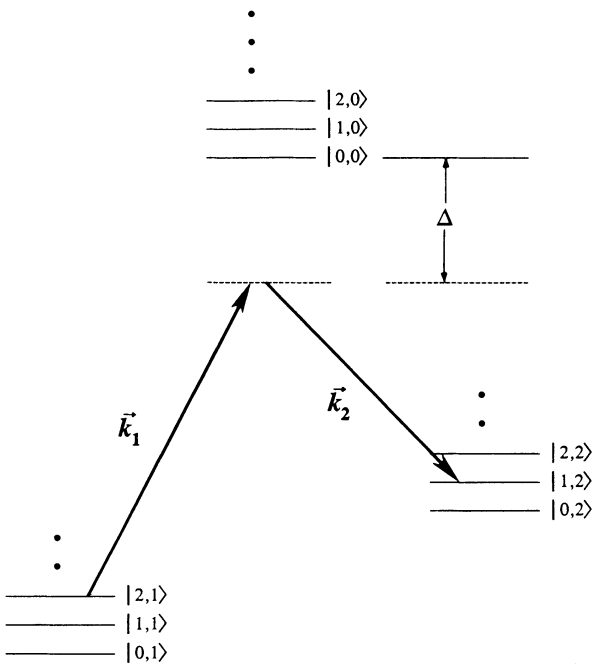

FIG. 10. Schematic representation of the energy levels for stimulated Raman transitions between internal (electronic) levels 1 and 2 of the trapped ion. The states are designated by the notation $|n,j\rangle$ where n denotes the ion harmonic-oscillator level and $j=0,1,2$ denotes the electronic state. $\mathbf{k}_1$ and $\mathbf{k}_2$ are the wave vectors for the traveling-wave fields which couple electronic level 0 to levels 1 and 2. We assume $\Delta \gg \omega_z$. In the figure, we schematically show the $|2,1\rangle \leftrightarrow |1,2\rangle$ stimulated Raman transition. Under the assumptions discussed in the text, the stimulated Raman transitions are equivalent to a Jaynes-Cummings-type coupling between electronic levels 1 and 2 and the harmonic (center-of-mass) motion of the ions.

are denoted by $|n,q\rangle = |n\rangle|q\rangle_e$ where n is the occupation number of the harmonic motion and $q=0,1,2$ denotes a particular electronic level. Decay from levels $|1\rangle_e$ and $|2\rangle_e$ is assumed to be negligible; level $|0\rangle_e$ decays at rate γ. The ions are irradiated by two laser beams with classical field amplitudes $\bar{E}_j = \mathrm{Re}\{\mathbf{E}_{0j}\exp[i(\mathbf{k}_j\cdot r - \omega_j t)]\}$ $(j=1,2)$ which couple level $|0\rangle_e$ to levels $|1\rangle_e$ and $|2\rangle_e$ with Rabi frequencies $g_{j0} \equiv |\boldsymbol{\mu}_{j0}\cdot\mathbf{E}_{0j}|/2\hbar$ where $\boldsymbol{\mu}_{0j}$ is the dipole matrix element between states $|0\rangle_e$ and $|j\rangle_e$. The frequencies of the beams are assumed to be equal to $\omega_1 = \omega_{01} - \Delta - \omega_z + \delta$ and $\omega_2 = \omega_{02} - \Delta$ where ω_{0j} is the transition frequency between states $|n,0\rangle$ and $|n,j\rangle$. We assume $\omega_{01}, \omega_{02} \gg \Delta \gg \omega_z \gg \delta$. The ions are initially prepared in the electronic state $|1\rangle_e$. When the ions are confined to the Lamb-Dicke limit (amplitude of motion $\ll 1/k_{jz}$ where $k_{jz} \equiv \mathbf{k}_j\cdot\hat{\mathbf{z}}$), a reduction in the harmonic-oscillator energy by $\hbar\omega_z$ occurs by stimulated Raman transitions $|n,1\rangle \rightarrow |n,0\rangle \rightarrow |n-1,2\rangle$ and $|n,1\rangle \rightarrow |n-1,0\rangle \rightarrow |n-1,2\rangle$ which reduce n by 1. In the second step of the cooling process, a laser tuned near ω_{02} causes spontaneous Raman transitions from level $|2\rangle_e$ back to $|1\rangle_e$. In the Lamb-Dicke limit, transitions of the form $|n-1,2\rangle \rightarrow |n-1,0\rangle \rightarrow |n-1,1\rangle$ are dominant in this second step. Therefore, after the two steps of the cooling process, $\langle n\rangle$ is reduced by 1. After repeated applications of this two-step process, the ions are eventually cooled until $\langle n\rangle \ll 1$ [18].

The first step of the cooling process realizes a Jaynes-Cummings coupling between the ions' harmonic oscillator and the internal levels $|1\rangle_e$ and $|2\rangle_e$. If we ensure the condition $\Delta \gg \pi\gamma/(2|\delta k_z| z_0 n^{1/2})$, where $\delta k_z \equiv k_{2z} - k_{1z}$, then the ions undergo stimulated Raman transitions with negligible probability of spontaneous decay from level $|0\rangle_e$ [18]. Under these conditions, the first step of the cooling process is adequately described by amplitude equations derived from Schrödinger equation. If we write the wave function for the system as

$$\Psi(t) = \sum_n \sum_{q=0}^{2} a_{n,q} e^{-i\omega_{n,q}t} |n,q\rangle \ , \tag{61}$$

then Schrödinger's equation leads to the amplitude equations [18]

$$da_{n,q}/dt = -\frac{i}{\hbar} \sum_{n'} \sum_{q'=0}^{2} a_{n,q} e^{i\omega_{n,q,n',q'}t} V_{n,q,n',q'} \ , \tag{62}$$

where $\hbar\omega_{n,q,n',q'}$ is the energy of state $|n,q\rangle$ minus the energy of state $|n',q'\rangle$ and $V_{n,q,n',q'}$ is the matrix element of the perturbation $-\boldsymbol{\mu}\cdot(\mathbf{E}_1+\mathbf{E}_2)$ between states $|n,q\rangle$ and $|n',q'\rangle$. If

$$|\omega_{10} - \omega_{20}| \gg \Delta \gg \gamma, g_{10}, g_{20}, \omega_z \ ,$$

we can adiabatically eliminate the excited states from the equations. With the additional assumption that $\omega_z \gg g_j^2/\Delta$, and neglecting terms in the equations of motion that vary with frequency ω_z or higher, we arrive at the amplitude equations

$$da_{n,1}/dt = i\Delta_{S1} a_{n,1} - \Omega^* n^{1/2} e^{i\delta t} a_{n-1,2} \tag{63}$$

and

$$da_{n-1,2}/dt = i\Delta_{S2} a_{n-1,2} + \Omega^* n^{1/2} e^{-i\delta t} a_{n,1} \ , \tag{64}$$

where $\Omega^* \equiv g_{10} g_{20} \delta k_z z_0/\Delta$, $\Delta_{S1} = g_{10}^2/\Delta$, and $\Delta_{S2} = g_{20}^2/\Delta$. The first terms in these equations are due to the ac Stark shifts of levels $|1\rangle_e$ and $|2\rangle_e$ by lasers 1 and 2, respectively. If $\Delta \gg |\omega_{10} - \omega_{20}|$, we have $\Delta_{S1} = (g_{10}^2 + g_{12}^2)/\Delta$, and $\Delta_{S2} = (g_{20}^2 + g_{21}^2)/\Delta$, where $g_{12} \equiv |\boldsymbol{\mu}_{10}\cdot\mathbf{E}_{02}|/2\hbar$ and $g_{21} \equiv |\boldsymbol{\mu}_{20}\cdot\mathbf{E}_{01}|/2\hbar$. We can now make the transformations $a_{n,1} = iA_{n,1}\exp(i\Delta_{S1}t)$ and $a_{n,2} = A_{n,2}\exp(i\Delta_{S2}t)$. If we let $\delta = \Delta_{S1} - \Delta_{S2}$, the equations of motion become

$$dA_{n,1}/dt = i\Omega^* n^{1/2} A_{n-1,2} \tag{65}$$

and

$$dA_{n-1,2}/dt = i\Omega^* n^{1/2} A_{n,1} \ . \tag{66}$$

The choice of δ is that which compensates for the differential ac Stark shifts in levels $|1\rangle_e$ and $|2\rangle_e$ and makes $\omega_1 - \omega_2$ resonant with the first lower motional sideband of the stimulated Raman transition. These equations are identical to Eqs. (57) (for $J=\frac{1}{2}$) if we make the identification $A_{n,1} \leftrightarrow C_{n,-1/2}$ and $A_{n,2} \leftrightarrow C_{n,+1/2}$; that is, if we identify the $|1\rangle_e$ and $|2\rangle_e$ states of Fig. 10 with the

$|-\rangle$ and $|+\rangle$ states of the spin-$\frac{1}{2}$ model. Hence, when spontaneous Raman transitions can be neglected, the system of Fig. 10 gives rise to the Jaynes-Cummings model coupling between the two-level system consisting of states $|1\rangle_e$ and $|2\rangle_e$, and the z c.m. harmonic motion of the ions. This causes Rabi oscillations between states $|n,1\rangle$ and $|n-1,2\rangle$ at frequency $\Omega^* n^{1/2}$.

To indicate possible experimental parameters, we consider the $^2S_{1/2}(F=1)\rightarrow{}^2P_{1/2}\rightarrow{}^2S_{1/2}(F=2)$ stimulated Raman transition in $^9Be^+$ ($\lambda=313$ nm, $\omega_{20}-\omega_{10}=1.25$ GHz). If we assume $|\delta k_z|=|k_z|$, $\omega_z/2\pi=5$ MHz, $g_{10}=g_{20}=750$ MHz, $\Delta/2\pi=20$ GHz, we find $|\delta k_z z_0|\simeq 0.21$, $\Omega^*/2\pi\simeq 150$ kHz, and the probability of spontaneous emission from the excited state during the time for complete transfer from the $F=1$ to $F=2$ ground state [18] to be approximately 0.01. If we assume that $\mu_{10}=\mu_{20}=q(0.5\times 10^{-8}$ cm) where q is the electron charge and that the ions are at the center of Gaussian laser beams with waist $w_0=20$ μm, then we require approximately 325 μW in each beam.

Realizations of the Jaynes-Cummings model using optical transitions are potentially interesting because the coupling frequencies Ω may be much higher than that provided by inhomogeneous magnetic fields acting on electron spins. In addition, lasers may allow spin squeezing to be applied to atomic levels which are of more interest for atomic clocks, such as hyperfine and optical transitions.

IX. SUMMARY AND DISCUSSION

In this paper, we have discussed the application of correlated particle states, or squeezed-spin states, to spectroscopy. Spin squeezing in other contexts has been discussed elsewhere [25–37]. This work extends that of a previous paper which introduced some of the ideas [38]. Transitions are assumed to be excited by classical radiation and detected by observing changes in the state populations of the particles (population spectroscopy). In this case, the fundamental limiting noise is projection noise [40], the noise associated with the quantum fluctuations in the measurement of populations. We find that the signal-to-noise ratio can be improved over the case of initially uncorrelated particles if the particles are first prepared in particular quantum-mechanically correlated or squeezed-spin states. We have considered a particular case of Ramsey's separated-oscillatory-field method of spectroscopy [41] since it gives the narrowest linewidth for a given interaction time. We introduce a squeezing parameter ξ_R which is the ratio of the uncertainty in the determination of the resonance frequency when using correlated states vs that when using uncorrelated states. This squeezing parameter has more general applicability, in that it gives a measure of the sensitivity of angular-momentum states to rotation. Since one description of interferometers is formally equivalent to Ramsey spectroscopy, the squeezing parameter might also be used in that context. Other squeezing parameters which are relevant in other contexts can be defined. We discussed certain states which exhibit a squeezing $\xi_R\simeq N^{-1/2}$. Because of our experimental background in the spectroscopy of stored atomic ions, we have investigated possible experimental schemes which might yield $\xi_R<1$ in this system.

The investigation and demonstration of squeezed-spin states is interesting for various reasons. These studies extend the realm of squeezing beyond the electromagnetic field. The ideas apply, in principle, to particle interferometry [29–31,35,36] and spectroscopy. From the practical side, since some trapped-ion spectroscopy experiments are currently limited by projection noise [40], the use of squeezed-spin states would yield more precise measurements. As a byproduct of these investigations we have discussed some schemes where it might be possible to realize the Jaynes-Cummings model [58] by coupling atomic internal levels to harmonic particle motion. In practice, this might allow the study of this fundamental quantum system and related cavity-QED experiments in the regime of weak relaxation and high detection efficiency. Also, it may be possible to generate correlated states which would be useful in multiparticle EPR experiments [2,38].

In spectroscopy, if we assume that the state preparation and detection time are small compared to the Ramsey interrogation time T, and if the measurement noise is limited by projection noise, the measurement uncertainty of the particle's transition frequency ω_0, expressed fractionally, is [76]

$$\frac{\Delta\omega}{\omega_0}=\frac{\xi_R}{\omega_0(\tau NT)^{1/2}}\ , \tag{67}$$

where $\tau\gg T$ is the total measurement time and ξ_R accounts for the use of correlated states. In a particular application, if we require a certain fractional frequency-measurement precision and if N and T are fixed, then the time τ required to reach this measurement precision is proportional to ξ_R^2. The reduction in measurement time due to $\xi_R<1$ would be particularly important in many applications using atomic clocks, where, to reach the highest measurement precision, the frequency is averaged over very long times, perhaps years. For states with $\xi_R=N^{-1/2}$, the required measurement time would be reduced by N.

We emphasize the importance of setting and maintaining the phase relationship between the fields which prepare the squeezed-spin states and the Ramsey fields. In the case where the squeezed-spin state is prepared by coupling to a harmonic oscillator, we must maintain the correct phase relationship between the oscillation of the harmonic oscillator, the coupling Ω at frequency ω_m, and the Ramsey fields. When we start from a squeezed-vacuum state of the harmonic oscillator, slight phase errors will increase the value of ξ_R that is obtained, but should not affect the accuracy of the measurement since the correlated state that is created should have $\langle J_y(0)\rangle=0$ [see Eq. (18)]. However, in the case where the squeezed-spin state is created from a coherent harmonic oscillator, it may be difficult to ensure that $\langle J_y(0)\rangle=0$. The resulting offset in the Ramsey curve would affect the accuracy (that is, it would give a systematic offset in our determination of ω_0), but if the offset

can be maintained constant it will not affect the relative measurement precision attained.

After the particles are put in squeezed-spin states, the correlations exist even though the particles do not interact. During the application of the squeezing Hamiltonian, the particles interact through their mutual coupling to the quantized harmonic oscillator(s). After this preparation stage, the particles do not interact even though the correlations remain. When the final particle states are measured, these correlations between particles are manifested even though, as in the classic EPR experiment, the particles have no way of "communicating" between one another.

In Sec. V C, we noted that it may be necessary to work with states that are not maximally squeezed since, when ξ_R reaches its minimum value, the signal also approaches 0 [for example, $\theta \rightarrow 0$ in Eq. (34)]. However, we can recover the advantages of squeezing without losing the signal by using a different measurement strategy. We can accomplish this by measuring higher moments of J_z. As an example, we consider measuring J_z^2 rather than J_z (or N_+) [38,77]. We illustrate the idea for $N=2$ ($J=1$). Let $\psi(0)=|1,0\rangle$. Using Eq. (24) we obtain

$$\langle J_z^2(t_f)\rangle = \sin^2\omega_r T \tag{68}$$

and

$$\Delta(J_z^2(t_f)) = \tfrac{1}{2}\sin 2\omega_r T \ . \tag{69}$$

As a function of ω (or ω_r), $\langle J_z^2(t_f)\rangle$ oscillates twice as fast as $\langle J_z(t_f)\rangle$ [in Eq. (14)]. In analogy with Eq. (13), the frequency imprecision for a single measurement is given by

$$|\Delta\omega| = \Delta(J_z^2(t_f))/|\partial\langle J_z^2(t_f)\rangle/\partial\omega| = 1/2T \ , \tag{70}$$

which is independent of ω. Therefore, effectively, $\xi_R = 1/\sqrt{2}$ ($=1/\sqrt{N}$) is obtained. For states of higher J, the maximum sensitivity may be given by measuring higher moments or combinations of higher moments.

Although we are most interested in states which exhibit quantum correlations between different particles, some of the interesting features and spectroscopic advantages of squeezed states can be studied in a different model system. In particular, consider an individual atom with $J > \frac{1}{2}$. As a concrete example assume $J=1$, as in the $^2S_{1/2}$ ($F=1$) ground hyperfine state of $^{199}Hg^+$. Suppose we are interested in measuring the Zeeman transition frequency for $\Delta M_F = \pm 1$ transitions when the ion is placed in a weak magnetic field. By weak, we mean a field where the Zeeman energy is much smaller than the ground-state hyperfine frequency, so the Zeeman sublevels are split equally. Suppose the ion is prepared in the $|F=1, M=0\rangle$ state. This state is equivalent to the squeezed state of Eq. (34) for $\theta \rightarrow 0$. We then apply radiation which drives the ion from the $|1,0\rangle$ state to the $|1,1\rangle$ and $|1,-1\rangle$ states. We can measure J_z^2, after application of the Zeeman radiation, by measuring the probability that the ion is detected to be in the $|1,0\rangle$ state by methods similar to those of Refs. [40] and [68]. As outlined in the last paragraph, this effectively gives $\xi_R = 2^{-1/2}$. One possible application of spin squeezing within a Zeeman level is for improved signal-to-noise ratio in electric-dipole-moment (EDM) experiments [77].

Several issues need further investigation. For example, we have not proved that, for a given measurement time T, the minimum value of $\Delta\omega$ is obtained for the particular method of spectroscopy we have assumed. Even for this method, other states may more closely approach the lower limit of $\xi_R = N^{-1/2}$ than the particular Rashid states investigated by Agarwal and Puri [34]. In considering the parametrically pumped oscillator [Eq. (59)], we have not optimized the squeezing for initial conditions or form of $\Omega_P(t)$. In considering the application of H_1 (or H_2), we have not considered all possible initial conditions, interaction times, or forms of $\Omega(t)$.

In all that we have discussed, we have assumed wave functions constructed with $|J,M\rangle$ basis states where $J=N/2$. This is because, prior to preparation of the spin-squeezed states, we assume initial states of the form $|J=N/2,M\rangle$, and the generators for the squeezed states preserve J. For completeness, we should consider similar basis states with $J<N/2$. Since, in general, ξ_R is larger for smaller values of J, we suspect that the smallest values of ξ_R are obtained for states with $J=N/2$.

In the spectroscopy we have described, we have assumed that, once the initial states are prepared, transitions are driven by classical fields. It will be interesting to investigate the signal-to-noise ratio when the spectroscopy is performed with quantized fields. In this case, we could consider both the case where transitions are detected by observing changes in state population and when they are detected by looking at changes in the transmitted or scattered radiation.

From the experimental side, we are hopeful that simpler practical ways can be found to generate spin squeezing than the schemes we have discussed. Nevertheless, even if states with only modest squeezing could be produced they would be very important in spectroscopy and perhaps other applications.

ACKNOWLEDGMENTS

We gratefully acknowledge the support of ONR. We thank G. S. Agarwal for sending a prepublication copy of Ref. [34]. We thank C. Monroe, J. Tan, M. Young, and P. Zoller for critical comments on the manuscript.

[1] A. Einstein, B. Podolsky, and N. Rosen, Phys. Rev. **47**, 777 (1935).

[2] For a recent review, see D. M. Greenberger, M. A. Horne, and A. Zeilinger, Phys. Today **46** (8), 22 (1993), and references therein.

[3] We note the EPR experiment using protons reported by M. Lamehi-Rachti and W. Mittig, Phys. Rev. D **14**, 2543 (1976), and the recently proposed experiment using correlated Hg atoms: E. Fry, in *Lasers '92*, Proceedings of the International Conference, Houston, TX, edited by C. P.

Wang (STS, McLean, VA, 1993), p. 621. See also the earlier review by J. F. Clauser and A. Shimony, Rep. Prog. Phys. **41**, 1881 (1978).

[4] J. Opt. Soc. Am. B **4**, 1450–1741 (1987), special issue on squeezed states of the electromagnetic field, edited by H. J. Kimble and D. F. Walls.

[5] J. Mod. Opt. **34**, 709–1020 (1987), special issue on squeezed light, edited by R. Loudon and P. L. Knight.

[6] H. J. Kimble, in *Fundamental Systems in Quantum Optics,* Proceedings of the Les Houches Summer School of Theoretical Physics, Session LIII, Les Houches, France, 1990, edited by J. Dalibard, J. M. Raimond, and J. Zinn-Justin (Elsevier, Amsterdam, 1992), p. 545.

[7] S. Reynaud, A. Heidmann, E. Giacobino, and C. Fabre, in *Progress in Optics,* edited by E. Wolf (North-Holland, Amsterdam, 1992), Vol. 30, pp. 3–85.

[8] M. Xiao, L. A. Wu, and H. J. Kimble, Phys. Rev. Lett. **59**, 278 (1987).

[9] P. Grangier, R. E. Slusher, B. Yurke, and A. LaPorta, Phys. Rev. Lett. **59**, 2153 (1987).

[10] E. S. Polzik, J. Carri, and H. J. Kimble, Phys. Rev. Lett. **68**, 3020 (1992).

[11] C. M. Caves, K. S. Thorne, R. W. P. Drever, V. D. Sandberg, and M. Zimmermann, Rev. Mod. Phys. **52**, 341 (1980).

[12] V. B. Braginsky, Y. I. Vorontsov, and K. S. Thorne, Science **209**, 547 (1980).

[13] F. Diedrich, J. C. Bergquist, W. M. Itano, and D. J. Wineland, Phys. Rev. Lett. **62**, 403 (1989).

[14] P. Verkerk, B. Lounis, C. Salomon, C. Cohen-Tannoudji, J.-Y. Courtois, and G. Grynberg, Phys. Rev. Lett. **68**, 3861 (1992).

[15] P. S. Jessen, C. Gerz, P. D. Lett, W. D. Phillips, S. L. Rolston, R. J. C. Spreeuw, and C. I. Westbrook, Phys. Rev. Lett. **69**, 49 (1992).

[16] A. Hemmerich and T. W. Hänsch, Phys. Rev. Lett. **70**, 410 (1993).

[17] J. C. Bergquist, F. Diedrich, W. M. Itano, and D. J. Wineland, in *Laser Spectroscopy IX,* edited by M. S. Feld, J. E. Thomas, and A. Mooradian (Academic, San Diego, 1989), p. 274.

[18] D. J. Heinzen and D. J. Wineland, Phys. Rev. A **42**, 2977 (1990).

[19] J. I. Cirac, A. S. Parkins, R. Blatt, and P. Zoller, Phys. Rev. Lett. **70**, 556 (1993).

[20] B. Baseia, R. Vyas, and V. S. Bagnato, Quantum Opt. **5**, 155 (1993).

[21] H. Zeng and F. Lin, Phys. Rev. A **48**, 2393 (1993).

[22] S. E. Harris, Phys. Rev. Lett. **62**, 1033 (1989); E. S. Fry, X. Li, D. Nikonov, G. G. Padmabandu, M. O. Scully, A. V. Smith, F. K. Tittel, C. Wang, S. R. Wilkinson, and S.-Y. Zhu, *ibid.* **70**, 3253 (1993); W. E. van der Veer, R. J. J. van Diest, A. Dönszelmann, and H. B. van Linden van den Heuvell, *ibid.* **70**, 3243 (1993), and references therein.

[23] D. Bohm, *Quantum Theory* (Prentice-Hall, Englewood Cliffs, NJ, 1951), p. 611.

[24] R. P. Feynman, F. L. Vernon, Jr., and R. W. Hellwarth, J. Appl. Phys. **28**, 49 (1957).

[25] M. A. Rashid, J. Math. Phys. **19**, 1391 (1978); **19**, 1397 (1978).

[26] D. F. Walls and P. Zoller, Phys. Rev. Lett. **47**, 709 (1981).

[27] K. Wodkiewicz and J. Eberly, J. Opt. Soc. Am. B **2**, 458 (1985); P. K. Aravind, *ibid.* **5**, 1545 (1988).

[28] J. D. Macomber and R. Lynch, J. Chem. Phys. **83**, 6514 (1985).

[29] B. Yurke, S. L. McCall, and J. R. Klauder, Phys. Rev. A **33**, 4033 (1986).

[30] B. Yurke, Phys. Rev. Lett. **56**, 1515 (1986).

[31] B. Yurke and E. A. Whittaker, Opt. Lett. **12**, 236 (1987).

[32] S. M. Barnett and M.-A. Dupertuis, J. Opt. Soc. Am. B **4**, 505 (1987).

[33] G. S. Agarwal and R. R. Puri, Phys. Rev. A **41**, 3782 (1990).

[34] G. S. Agarwal and R. R. Puri, Phys. Rev. A (to be published).

[35] M. Kitagawa and M. Ueda, Phys. Rev. Lett. **67**, 1852 (1991); in *Noise in Physical Systems and* $1/f$ *Fluctuations,* edited by T. Musha, S. Sato, and M. Yamamoto (Ohmsha, Tokyo, 1991), p. 355.

[36] M. Kitagawa and M. Ueda, Phys. Rev. A **47**, 5138 (1993).

[37] G. S. Agarwal, J. P. Dowling, and W. P. Schleich, in *Proceedings of the Second Workshop on Squeezed States and Uncertainty Relations, Moscow, 1992,* edited by Y. S. Kim and V. I. Man'ko (NASA, Goddard Spaceflight Center, in press).

[38] D. J. Wineland, J. J. Bollinger, W. M. Itano, F. L. Moore, and D. J. Heinzen, Phys. Rev. A **46**, R6797 (1992).

[39] *Trapped Ions and Laser Cooling III,* edited by J. C. Bergquist, J. J. Bollinger, W. M. Itano, and D. J. Wineland, Natl. Inst. Stand. Technol. (U.S.) Tech. Note No. 1353 (U.S. GPO, Washington, DC, 1992).

[40] W. M. Itano, J. C. Bergquist, J. J Bollinger, J. M. Gilligan, D. J. Heinzen, F. L. Moore, M. G. Raizen, and D. J. Wineland, Phys. Rev. A **47**, 3554 (1993).

[41] N. F. Ramsey, *Molecular Beams* (Oxford University, London, 1963).

[42] C. K. Hong, S. R. Friberg, and L. Mandel, Appl. Opt. **24**, 3877 (1985).

[43] A. Heidmann, R. J. Horowicz, S. Reynaud, E. Giacobino, C. Fabre, and G. Camy, Phys. Rev. Lett. **59**, 2555 (1987).

[44] M. Xiao, L.-A. Wu, and H. J. Kimble, Opt. Lett. **13**, 476 (1988).

[45] C. D. Nabors and R. M. Shelby, Phys. Rev. A **42**, 556 (1990).

[46] P. R. Tapster, S. F. Seward, and J. G. Rarity, Phys. Rev. A **44**, 3266 (1991).

[47] R. H. Dicke, Phys. Rev. **93**, 99 (1954).

[48] F. T. Arecchi, E. Courtens, R. Gilmore, and H. Thomas, Phys. Rev. A **6**, 2211 (1972).

[49] In Ref. [38], we transformed to a frame rotating at ω_0.

[50] J. J. Bollinger, J. D. Prestage, W. M. Itano, and D. J. Wineland, Phys. Rev. Lett. **54**, 1000 (1985); J. J. Bollinger, D. J. Heinzen, W. M. Itano, S. L. Gilbert, and D. J. Wineland, *ibid.* **63**, 1031 (1989).

[51] From the form of Eq. (14), it is only possible to determine ω_0 modulo $2\pi/(lT)$ where l is an integer. Experimentally, the "central lobe" of the Ramsey pattern is identified by varying T and observing which lobe is stationary, or using the Rabi resonance method (B_1 constant from $t=0$ to t_f) which gives a (lower-resolution) resonance curve peaked at ω_0.

[52] A choice of $n>0$ can be experimentally useful to test for any systematic effects associated with the power of the clock radiation.

[53] For a choice of $n>0$, it is possible to investigate experimentally a class of systematic effects, such as the presence of a systematic term of the form $K_s(\omega-\omega_0)$ (K_s a constant) which adds to the signal $\langle N_+(t_f)\rangle$ given in Eq. (14).

This "background slope" effect can be accounted for by determining ω_0 for various values of n, which effectively measures K_s.

[54] A. Messiah, *Quantum Mechanics* (Wiley, New York, 1961).

[55] R. A. Campos, B. E. A. Saleh, and M. C. Teich, Phys. Rev. A **40**, 1371 (1989).

[56] These operators have also been considered earlier by J. Schwinger in a reformulated theory of angular momentum. See J. Schwinger, in *Quantum Theory of Angular Momentum,* edited by L. C. Biedenharn and H. van Dam (Academic, New York, 1965).

[57] A. Heidmann, J. M. Raimond, and S. Reynaud, Phys. Rev. Lett. **54**, 326 (1985).

[58] E. T. Jaynes and C. W. Cummings, Proc. IEEE **51**, 89 (1963).

[59] W. H. Press, B. P. Flannery, S. A. Teukolsky, and W. T. Vetterling, *Numerical Recipes* (Cambridge University, New York, 1986), p. 547.

[60] See, for example, R. W. Henry and S. C. Glotzer, Am. J. Phys. **56**, 318 (1988).

[61] C. W. Gardiner, Phys. Rev. Lett. **56**, 1917 (1986); A. S. Parkins and C. W. Gardiner, Phys. Rev. A **40**, 3796 (1989).

[62] S. Haroche and J. M. Raimond, Adv. At. Mol. Phys. **20**, 347 (1985).

[63] S. Haroche, M. Brune, and J. M. Raimond, in *Atomic Physics 12,* edited by J. C. Zorn and R. R. Lewis (AIP, New York, 1991), p. 204; S. Haroche, in *Fundamental Systems in Quantum Optics* (Ref. [6]), p. 767.

[64] G. Rempe, M. O. Scully, and H. Walther, in *Atomic Physics 12* (Ref. [63]), p. 219.

[65] H. G. Dehmelt, Adv. At. Mol. Phys. **3**, 53 (1967); **5**, 109 (1969).

[66] D. J. Wineland and H. G. Dehmelt, J. Appl. Phys. **46**, 919 (1975).

[67] H. Dehmelt, Science **247**, 539 (1990).

[68] M. G. Raizen, J. M. Gilligan, J. C. Bergquist, W. M. Itano, and D. J. Wineland, Phys. Rev. A **45**, 6493 (1992).

[69] This coupling was previously considered in a cooling scheme discussed by H. Harde, in *International Conference on Quantum Electronics Technical Digest Series 1990* (Optical Society of America, Washington, DC, 1990), Vol. 8, p. 278.

[70] C. A. Blockley, D. F. Walls, and H. Risken, Europhys. Lett. **17**, 509 (1992).

[71] J. I. Cirac, R. Blatt, A. S. Parkins, and P. Zoller, Phys. Rev. Lett. **70**, 762 (1993).

[72] H. Dehmelt, G. Janik, and W. Nagourney, Bull. Am. Phys. Soc. **30**, 111 (1985).

[73] M. Lindberg and J. Javanainen, J. Opt. Soc. Am. B **3**, 1008 (1986).

[74] P. E. Toschek and W. Neuhauser, J. Opt. Soc. Am. B **6**, 2220 (1989).

[75] M. Kasevich and S. Chu, Phys. Rev. Lett. **69**, 1741 (1992).

[76] D. J. Wineland, W. M. Itano, J. C. Bergquist, J. J. Bollinger, S. L. Gilbert, and F. Diedrich, in *Frequency Standards and Metrology,* Proceedings of the Fourth Symposium on Frequency Standards and Metrology, Ancona, Italy, 1988, edited by A. De Marchi (Springer-Verlag, Berlin, Heidelberg, 1989), p. 71.

[77] This measurement scheme has been used in other experiments. See, for example, K. Abdullah, C. Carlberg, E. D. Commins, H. Gould, and S. B. Ross, Phys. Rev. Lett. **65**, 2347 (1990). The noise in that experiment, however, was not dominated by projection noise.